IPHE 2002-011
September 11 2002

CP VIOLATION

Current status and future prospect

Lecture given at
Vth Moscow School of Physics
XXXth ITEP Winter School of Physics
Moscow, Russia, February, 2002

T. Nakada

CERN EP-Division
CH-1211 Geneva 23, Switzerland
and
Institute of High Energy Physics, University of Lausanne
CH-1015 Lausanne, Switzerland

(On leave from PSI, CH-5232 Villigen-PSI, Switzerland)

1 Introduction

Parity violation was discovered in 1957 in nuclear β decays [1] and pion and muon decays [2]. In the charged current interaction of the standard electroweak theory, parity and charge conjugation symmetries are maximally violated due to the $V - A$ structure [3]. All the experimental results up to now are in full agreement with the theory.

A surprising discovery of the CP violating $\mathrm{K_L} \to \pi^+\pi^-$ decays [4] was made in 1964. Since then, CP violation has been observed in various decay modes of the neutral kaon. In 2001, CP violation was seen first time out side of the neutral kaon system in the decays on neutral B-mesons into $\mathrm{J}/\psi\mathrm{K_S}$ [5]. The Standard Model with three fermion families can accommodate all those observed CP violation phenomena through a complex quark mixing matrix [6], the Cabibbo-Kobayashi-Maskawa (CKM) matrix [6, 7]. However, due to the large uncertainties in evaluating the effect of hadronic interactions for some processes and limited number of measurements of CP violation, we cannot exclude a possibility that physics beyond the Standard Model makes a sizable contribution to CP violation in elementary particle physics.

Interest in CP violation is not limited to elementary particle physics. It is one of the three necessary ingredients to generate the observed excess of matter over antimatter in the universe [8]. The other two conditions are baryon number violation and being out of thermal equilibrium. It was realised [9] that the Standard Model could meet those three requirements: baryon number violation through transitions to different vacuum states above the electroweak energy scale, being out of thermal equilibrium at the electroweak energy scale through the first order phase transition, and CP violation through the Kobayashi-Maskawa phase in the CKM matrix. However, the current lower limit of the Higgs particle mass is already too high [10] to produce the first order phase transition. Furthermore, CP violation present in the Standard Model is far too small to explain the observed matter-antimatter asymmetry in the universe [11]. Baryogenesis at the electroweak energy scale is still possible in various extensions of the Standard Model, which introduce additional sources of CP violation. This provides a strong motivation to search for effects of new physics in CP violation.

For CP violation in some B meson decay channels, the Standard Model can make precise predictions with little influence from the strong interactions. Those channels can be used to test the predictions quantitatively to look for a sign of new physics. In addition, CP violation is expected in many decay modes in the B meson system. The pattern of CP violation allows us to make a systematic qualitative comparison with the Standard Model predictions. Therefore, it is now widely accepted that the B-meson system provides in future an ideal place for testing the Standard Model for CP violation [12]. In the neutral kaon system, there exists a decay mode, $\mathrm{K_L} \to \pi^0\nu\overline{\nu}$

where the effect of CP violation can be predicted by the Standard Model with little theoretical uncertainty. This could certainly provide complementary information to test the Standard Model.

In this article, we first derive the formalism [13] describing the particle-antiparticle system, with and without CP violation. Three different mechanisms which can generate CP violation are clearly classified, together with experimental observables which identify contributions from the different mechanisms. Then, CP violation in the neutral kaon system is analysed in this formalism. After a brief discussion on the Standard Model description for CP violation in the neutral kaon system, we proceed to the neutral B meson system. Some Standard Model predictions are described and it is discussed how the situation could change if new physics existed and contributed to the B meson system. The latest experimental results are presented.

2 Description of a Particle-Antiparticle System

2.1 Basic Formalism

CP (charge conjugation and parity transformation) is a unitary transformation. Arbitrary ket-vectors, $|\alpha\rangle$ and $|\beta\rangle$, and the CP transformed ones,

$$CP\,|\alpha\rangle \equiv |\alpha_{\rm CP}\rangle \quad \text{and} \quad CP\,|\beta\rangle \equiv |\beta_{\rm CP}\rangle\ ,$$

satisfy

$$\langle\alpha_{\rm CP}|\beta_{\rm CP}\rangle = \langle\alpha|\beta\rangle,$$

i.e.

$$\left[\langle\alpha|(CP)^\dagger\right] CP|\beta\rangle = \langle\alpha|\left[(CP)^\dagger CP|\beta\rangle\right] = \langle\alpha|\beta\rangle$$

which implies

$$(CP)^\dagger CP = \mathbf{1}.$$

T (time reversal) is an antiunitary operator. The relation between arbitrary ket-vectors, $|\alpha\rangle$ and $|\beta\rangle$, and the T transformed ones,

$$T\,|\alpha\rangle \equiv |\alpha_{\rm T}\rangle \quad \text{and} \quad T\,|\beta\rangle \equiv |\beta_{\rm T}\rangle\ ,$$

is given by

$$\langle\alpha_{\rm T}|\beta_{\rm T}\rangle = \left(\langle\alpha|T^\dagger\right) T|\beta\rangle = \left(\langle\alpha|\beta\rangle\right)^*.$$

It follows that,

$$\left(\langle\alpha|T^\dagger\right) T|\beta\rangle = \left[\langle\alpha|\left(T^\dagger T|\beta\rangle\right)\right]^*$$

and

$$T^\dagger T = \mathbf{1}.$$

Note that an expression must be complex-conjugated when the direction to which T operator acts is changed.

We now examine how T commutes with an arbitrary complex number c. By introducing $Tc = c'T$, it follows that

$$\begin{aligned} c\langle\alpha|\alpha\rangle &= \langle\alpha|c|\alpha\rangle \\ &= \langle\alpha|\left(T^\dagger T c T^\dagger T|\alpha\rangle\right) \\ &= \left[\left(\langle\alpha|T^\dagger\right)\left(TcT^\dagger T|\alpha\rangle\right)\right]^* \\ &= \left[\langle\alpha_{\rm T}|\ \left(T\,c\,T^\dagger\ |\alpha_{\rm T}\rangle\right)\right]^* \\ &= \left[\langle\alpha_{\rm T}|c'\ \left(TT^\dagger|\alpha_{\rm T}\rangle\right)\right]^* \\ &= c'^*\left(\langle\alpha_{\rm T}|\alpha_{\rm T}\rangle\right)^* \\ &= c'^*\langle\alpha|\alpha\rangle \end{aligned}$$

thus $c' = c^*$ and

$$T\,c = c^*\,T.$$

In a similar way, we can derive

$$CP\,c = c\,CP\ .$$

Let $|{\rm P}^0\rangle$ and $|\overline{\rm P}^0\rangle$ be the states of a neutral pseudoscalar particle ${\rm P}^0$ and its antiparticle $\overline{\rm P}^0$ at rest, respectively. They have definite flavour quantum numbers with opposite signs: $F = +1$ for ${\rm P}^0$ and $F = -1$ for $\overline{\rm P}^0$. Both states are eigenstates of the strong and electromagnetic interaction Hamiltonian, i.e.

$$(H_{\rm st} + H_{\rm em})\,|{\rm P}^0\rangle = m_0|{\rm P}^0\rangle \quad\text{and}\quad (H_{\rm st} + H_{\rm em})\,|\overline{\rm P}^0\rangle = \overline{m}_0|\overline{\rm P}^0\rangle \tag{1}$$

where m_0 and $\overline{m}_0$ are the rest masses of ${\rm P}^0$ and $\overline{\rm P}^0$, respectively. The ${\rm P}^0$ and $\overline{\rm P}^0$ states are related through CP transformations. For stationary states, the T transformation does not alter them, with the exception of an arbitrary phase. In summary, we obtain

$$\begin{gathered} CP\,|{\rm P}^0\rangle = e^{i\,\theta_{\rm CP}}|\overline{\rm P}^0\rangle \quad\text{and}\quad CP\,|\overline{\rm P}^0\rangle = e^{-\,i\,\theta_{\rm CP}}|{\rm P}^0\rangle \\ T\,|{\rm P}^0\rangle = e^{i\,\theta_{\rm T}}|{\rm P}^0\rangle \quad\text{and}\quad T\,|\overline{\rm P}^0\rangle = e^{i\,\overline{\theta}_{\rm T}}|\overline{\rm P}^0\rangle \end{gathered} \tag{2}$$

where the θ's are arbitrary phases, and by requiring $CPT\,|{\rm P}^0\rangle = TCP\,|{\rm P}^0\rangle$ it follows that

$$2\,\theta_{\rm CP} = \overline{\theta}_{\rm T}\ -\ \theta_{\rm T}\ . \tag{3}$$

If strong and electromagnetic interactions are invariant under the CPT transformation, which is assumed throughout this paper,

$$CPT\,(H_{\rm st} + H_{\rm em})\,(CPT)^{-1} = H_{\rm st} + H_{\rm em}\ ,$$

it follows that

$$\begin{aligned} m_0 &= \langle \mathrm{P}^0|(H_{\mathrm{st}}+H_{\mathrm{em}})|\mathrm{P}^0\rangle \\ &= \langle \mathrm{P}^0|\left[(CPT)^{-1}\,CPT\,(H_{\mathrm{st}}+H_{\mathrm{em}})\,(CPT)^{-1}\,CPT|\mathrm{P}^0\rangle\right] \\ &= \left\{\left[\langle \mathrm{P}^0|(CPT)^{-1}\right]\,(H_{\mathrm{st}}+H_{\mathrm{em}})\,\left[CPT|\mathrm{P}^0\rangle\right]\right\}^* \ . \end{aligned}$$

Using Equations 1 and 2, we obtain

$$m_0 = \overline{m}_0 \ ,$$

i.e. the rest mass of a particle and that of its antiparticle are identical.

Now we switch on the weak interaction, V, through which P can decay into final states f with different flavours ($|\Delta F| = 1$ process) and P^0 and $\overline{\mathrm{P}}^0$ can oscillate to each other ($|\Delta F| = 2$ process). Thus, any state $|\psi(t)\rangle$ which is a solution of the Schrödinger equation

$$i\,\frac{\partial}{\partial t}|\psi(t)\rangle = (H_{\mathrm{st}}+H_{\mathrm{em}}+V)\,|\psi(t)\rangle \tag{4}$$

can be written as

$$|\psi(t)\rangle = a(t)|\mathrm{P}^0\rangle + b(t)|\overline{\mathrm{P}}^0\rangle + \sum_{\mathrm{f}} c_{\mathrm{f}}(t)|\mathrm{f}\rangle$$

where the sum is taken over all the possible final states f, which are both real and virtual, and $a(t)$, $b(t)$ and $c_{\mathrm{f}}(t)$ are time dependent functions; $|a(t)|^2$, $|b(t)|^2$ and $|c_{\mathrm{f}}(t)|^2$ give the fractions of P^0, $\overline{\mathrm{P}}^0$ and f at time t respectively.

By introducing

$$\begin{aligned} \tilde{a}(t) &= a(t)e^{i(H_{\mathrm{st}}+H_{\mathrm{em}})\,t} &(5)\\ \tilde{b}(t) &= b(t)e^{i(H_{\mathrm{st}}+H_{\mathrm{em}})\,t} &(6)\\ \tilde{c}_{\mathrm{f}}(t) &= c_{\mathrm{f}}(t)e^{i(H_{\mathrm{st}}+H_{\mathrm{em}})\,t} \end{aligned}$$

and

$$|\tilde{\psi}(t)\rangle = \tilde{a}(t)|\mathrm{P}^0\rangle + \tilde{b}(t)|\overline{\mathrm{P}}^0\rangle + \sum_{\mathrm{f}} \tilde{c}_{\mathrm{f}}(t)|\mathrm{f}\rangle$$

Equation 4 can be written as

$$i\,\frac{\partial}{\partial t}|\tilde{\psi}(t)\rangle = V(t)|\tilde{\psi}(t)\rangle \tag{7}$$

where $V(t) = e^{i(H_{\mathrm{st}}+H_{\mathrm{em}})\,t}Ve^{-i(H_{\mathrm{st}}+H_{\mathrm{em}})\,t}$. Note that V **does not commute** with $H_{\mathrm{st}}+H_{\mathrm{em}}$. By operating $\langle \mathrm{P}^0|$, $\langle\overline{\mathrm{P}}^0|$ and $\langle \mathrm{f}'|$ from the left side of Equation 7, we

obtain

$$i\,\frac{\partial}{\partial t}\tilde{a}(t) = \langle \mathrm{P}^0|V|\mathrm{P}^0\rangle\tilde{a}(t) + \langle \mathrm{P}^0|V|\overline{\mathrm{P}}^0\rangle\tilde{b}(t) + \sum_{\mathrm{f}}\langle \mathrm{P}^0|V|\mathrm{f}\rangle\tilde{c}_{\mathrm{f}}(t)e^{i(m_0-E_{\mathrm{f}})t} \tag{8}$$

$$i\,\frac{\partial}{\partial t}\tilde{b}(t) = \langle \overline{\mathrm{P}}^0|V|\mathrm{P}^0\rangle\tilde{a}(t) + \langle \overline{\mathrm{P}}^0|V|\overline{\mathrm{P}}^0\rangle\tilde{b}(t) + \sum_{\mathrm{f}}\langle \overline{\mathrm{P}}^0|V|\mathrm{f}\rangle\tilde{c}_{\mathrm{f}}(t)e^{i(m_0-E_{\mathrm{f}})t} \tag{9}$$

and

$$\begin{aligned} i\,\frac{\partial}{\partial t}\tilde{c}_{\mathrm{f}'}(t) &= \langle \mathrm{f}'|V|\mathrm{P}^0\rangle\tilde{a}(t)e^{i(E_{\mathrm{f}'}-m_0)t} + \langle \mathrm{f}'|V|\overline{\mathrm{P}}^0\rangle\tilde{b}(t)e^{i(E_{\mathrm{f}'}-m_0)t} \\ &\quad + \sum_{\mathrm{f}}\langle \mathrm{f}'|V|\mathrm{f}\rangle\tilde{c}_{\mathrm{f}'}(t)e^{i(E_{\mathrm{f}'}-E_{\mathrm{f}})t} \end{aligned} \tag{10}$$

By applying the Wigner-Weisskopf approximation [14], the last term of Equation 10, which is due to the weak interaction between the final states, can be neglected and partial integration of Equation 10 leads to

$$\tilde{c}_{\mathrm{f}'}(t) = \lim_{\epsilon\to+0}\frac{e^{i(E_{\mathrm{f}'}-m_0)t}}{m_0 - E_{\mathrm{f}'} + i\epsilon}\left[\langle \mathrm{f}'|V|\mathrm{P}^0\rangle\tilde{a}(t) + \langle \mathrm{f}'|V|\overline{\mathrm{P}}^0\rangle\tilde{b}(t)\right] + \mathcal{O}(V^2) \tag{11}$$

where the choice of $\epsilon > 0$ is made so that the expression remains finite for $t \to \infty$. Since the weak interaction is much weaker than strong and electromagnetic interactions, perturbation theory can be applied and terms with higher orders in V are neglected. By inserting Equation 11 into Equations 8 and 9, $\tilde{a}(t)$ and $\tilde{b}(t)$ are now decoupled from $\tilde{c}_{\mathrm{f}}(t)$.

Using the theorem

$$\lim_{\epsilon\to+0}\frac{1}{x+i\epsilon} = \mathcal{P}\left(\frac{1}{x}\right) - i\pi\delta(x)\ ,$$

where $\mathcal{P}$ stands for the principal part, and Equations 5 and 6, the original Schrödinger equation 4 is reduced to

$$i\,\frac{\partial}{\partial t}\begin{pmatrix} a(t) \\ b(t)\end{pmatrix} = \mathbf{\Lambda}\begin{pmatrix} a(t) \\ b(t)\end{pmatrix} = \left(\boldsymbol{M} - \,i\,\frac{\mathbf{\Gamma}}{2}\right)\begin{pmatrix} a(t) \\ b(t)\end{pmatrix} \tag{12}$$

where only $a(t)$ and $b(t)$ appear. The elements of the 2×2 matrices $\boldsymbol{M}$ (mass matrix) and $\mathbf{\Gamma}$ (decay matrix) are given as

$$M_{ij} = m_0\,\delta_{ij} + \langle i|V|j\rangle + \sum_{\mathrm{f}}\mathcal{P}\left(\frac{\langle i|V|\mathrm{f}\rangle\langle \mathrm{f}|V|j\rangle}{m_0 - E_{\mathrm{f}}}\right) \tag{13}$$

and

$$\Gamma_{ij} = 2\,\pi\sum_{\mathrm{f}}\langle i|V|\mathrm{f}\rangle\langle \mathrm{f}|V|j\rangle\delta(m_0 - E_{\mathrm{f}}) \tag{14}$$

respectively where the index $i = 1(2)$ denotes $\mathrm{P}^0(\overline{\mathrm{P}}^0)$. Note that the sum is taken over *all possible* intermediate states for the mass matrix, and only *real* final states are considered for the decay matrix. In this matrix representation, $|\mathrm{P}^0\rangle$ and $\overline{\mathrm{P}}^0\rangle$ are given by

$$|\mathrm{P}^0\rangle = \begin{pmatrix} 1 \\ 0 \end{pmatrix} \text{ and } |\overline{\mathrm{P}}^0\rangle = \begin{pmatrix} 0 \\ 1 \end{pmatrix} . \tag{15}$$

If the Hamiltonians are not Hermitian, transition probabilities are not conserved in decays or oscillations, i.e. the number of initial states is not identical to the number of final states. This is also referred to as the break down of unitarity. We assume from now on that all the Hamiltonians are Hermitian. Therefore, we have

$$|a(t)|^2 + |b(t)|^2 + \sum_{\mathrm{f}} |c_{\mathrm{f}}|^2 = 1,$$

and

$$M_{ij} = M^*_{ji},\ \Gamma_{ij} = \Gamma^*_{ji} ,$$

from Equations 13 and 14, noting $V^\dagger = V$. Clearly $|a(t)|^2 + |b(t)|^2$ decreases as a function of time, hence $\mathbf{\Lambda}$ is not Hermitian.

If V is invariant under the T transformation, i.e. $T\,V\,T^{-1} = V$, it follows that

$$\begin{aligned} \langle \mathrm{P}^0|V|\overline{\mathrm{P}}^0\rangle &= \langle \mathrm{P}^0| \left(T^{-1}T\,V\,T^{-1}T|\overline{\mathrm{P}}^0\rangle\right) \\ &= \left(\langle \mathrm{P}^0|V|\overline{\mathrm{P}}^0\rangle e^{2i\theta_{\mathrm{CP}}}\right)^* \\ &= \langle \overline{\mathrm{P}}^0|V^\dagger|\mathrm{P}^0\rangle e^{-2i\theta_{\mathrm{CP}}} \\ &= \langle \overline{\mathrm{P}}^0|V|\mathrm{P}^0\rangle e^{-2i\theta_{\mathrm{CP}}} \end{aligned}$$

and

$$\sum_{\mathrm{f}} \langle \mathrm{P}^0|V|\mathrm{f}\rangle\langle \mathrm{f}|V|\overline{\mathrm{P}}^0\rangle = \sum_{\mathrm{f_T}} \langle \overline{\mathrm{P}}^0|V|\mathrm{f_T}\rangle\langle \mathrm{f_T}|V|\mathrm{P}^0\rangle e^{-2i\theta_{\mathrm{CP}}} ,$$

where Equations 2 and 3 are used and $|\mathrm{f_T}\rangle = T|\mathrm{f}\rangle$. Since the sum is taken over all the final states with all the possible kinematical configurations, it can be shown that

$$\sum_{\mathrm{f}} |\mathrm{f}\rangle\langle \mathrm{f}| = \sum_{\mathrm{f_T}} |\mathrm{f_T}\rangle\langle \mathrm{f_T}| .$$

From Equations 13 and 14, we now obtain $\Lambda_{12} = \Lambda_{21} e^{-2i\theta_{\mathrm{CP}}}$: i.e.

$$\text{T conservation} \Longrightarrow |\Lambda_{12}| = |\Lambda_{21}| .$$

In a similar way, the following relations can be obtained if V is invariant under the CP transformation:

$$\text{CP conservation} \Longrightarrow |\Lambda_{12}| = |\Lambda_{21}| \text{ and } \Lambda_{11} = \Lambda_{22} .$$

By combining the two, we obtain for the CPT invariant case:

$$\text{CPT conservation} \Longrightarrow \Lambda_{11} = \Lambda_{22} \ .$$

It follows that

- if $\Lambda_{11} \neq \Lambda_{22}$, i.e. $M_{11} \neq M_{22}$ or $\Gamma_{11} \neq \Gamma_{22}$:
  CPT and CP are violated
- if $|\Lambda_{12}| \neq |\Lambda_{21}|$:
  T and CP are violated .

Note that CP violation cannot be separated from CPT violation and T violation.

While there is no fundamental reason to respect CP and T symmetries, it can be shown based on only a few very fundamental assumptions that no self-consistent quantum field theory can be constructed that does not conserve CPT symmetry [15]. Therefore, we restrict our further discussion to the case where **CPT symmetry is conserved**:

$$M_{11} = M_{22} \equiv M \text{ and } \Gamma_{11} = \Gamma_{22} \equiv \Gamma$$

so that

$$\Lambda_{11} = \Lambda_{22} \equiv \Lambda \ .$$

i.e.

$$\mathbf{\Lambda} = \begin{pmatrix} \Lambda & \Lambda_{12} \\ \Lambda_{21} & \Lambda \end{pmatrix} \tag{16}$$

where

$$\Lambda = M - \frac{i}{2}\Gamma, \ \Lambda_{12} = M_{12} - \frac{i}{2}\Gamma_{12}, \ \Lambda_{21} = M_{12}^* - \frac{i}{2}\Gamma_{12}^* \ .$$

Now Equation 12 can be written as

$$i\frac{\partial a(t)}{\partial t} = \Lambda\, a(t) + \Lambda_{12}\, b(t) \tag{17}$$

$$i\frac{\partial\, b(t)}{\partial t} = \Lambda_{21}\, a(t) + \Lambda\, b(t) \ . \tag{18}$$

Equation 17 implies

$$b(t) = \frac{1}{\Lambda_{12}}\left[i\,\frac{d\, a(t)}{dt} - \Lambda\, a(t) \right] \ . \tag{19}$$

By differentiating Equation 17 with respect to t, we obtain

$$i\frac{\partial^2 a(t)}{\partial t^2} = \Lambda\,\frac{\partial\, a(t)}{\partial\, t} + \Lambda_{12}\,\frac{\partial\, b(t)}{\partial\, t} \ .$$

Using Equations 18 and 19, it follows that

$$\frac{\partial^2 a(t)}{\partial t^2} + 2\,i\,\Lambda\,\frac{\partial\, a(t)}{\partial t} + \left(\Lambda_{12}\Lambda_{21} - \Lambda^2\right) a(t) = 0\ , \tag{20}$$

where a general solution of this differential equation is given by

$$a(t) = C_+ e^{-i\lambda_+ t} + C_- e^{-i\lambda_- t} \tag{21}$$

and $C_\pm$ are arbitrary constants which can only be defined by the initial condition. Then, $b(t)$ can be derived from Equation 19. Insertion of Equation 21 into Equation 20 leads to

$$\lambda_\pm^2 - 2\Lambda\lambda_\pm - \left(\Lambda_{12}\Lambda_{21} - \Lambda^2\right) = 0$$

from which the eigen-frequencies are obtained as

$$\lambda_\pm = \Lambda \pm \sqrt{\Lambda_{12}\Lambda_{21}}$$

For an initially pure P^0 state, we have $a(t) = 1$ and $b(t) = 0$ at $t = 0$, i.e. $C_+ = C_- = 1/2$. If we focus our interest only on $|\mathrm{P}^0\rangle$ and $|\overline{\mathrm{P}}^0\rangle$, the solution of Equation 4 becomes

$$\begin{aligned} |\mathrm{P}^0(t)\rangle &= a(t)|\mathrm{P}^0\rangle + b(t)|\overline{\mathrm{P}}^0\rangle \\ &= f_+(t)|\mathrm{P}^0\rangle + \zeta f_-(t)\,|\overline{\mathrm{P}}^0\rangle \qquad (22) \\ &= \frac{\sqrt{1+|\zeta|^2}}{2}\left(\,|\mathrm{P}_+\rangle\, e^{-\,i\,\lambda_+\,t} + |\mathrm{P}_-\rangle\, e^{-\,i\,\lambda_-\,t}\,\right) \qquad (23) \end{aligned}$$

where

$$f_\pm(t) = \frac{1}{2}\left(\,e^{-\,i\,\lambda_+\,t} \pm e^{-\,i\,\lambda_-\,t}\,\right)$$

and

$$\zeta = \sqrt{\frac{\Lambda_{21}}{\Lambda_{12}}}\ . \tag{24}$$

The two states $|\mathrm{P}_+\rangle$ and $|\mathrm{P}_-\rangle$ are given by

$$|\mathrm{P}_\pm\rangle = \frac{1}{\sqrt{1+|\zeta|^2}}\left(|\mathrm{P}^0\rangle \,\pm\, \zeta\,|\overline{\mathrm{P}}^0\rangle\right)\ . \tag{25}$$

and their matrix representation can be derived to be

$$|\mathrm{P}_\pm\rangle = \frac{1}{\sqrt{1+|\zeta|^2}}\begin{pmatrix} 1 \\ \pm\zeta \end{pmatrix}\ .$$

from Equation 15. Using this matrix representation and Equation 16, it follows that

$$\mathbf{\Lambda}|\mathrm{P}_\pm\rangle = \lambda_\pm|\mathrm{P}_\pm\rangle \ , \tag{26}$$

i.e. P_+ and P_- are the eigenstates of $\mathbf{\Lambda}$ with eigenvalues λ_+ and λ_- respectively.

It must be noted that Λ_{12} and Λ_{21} are complex numbers, thus ζ has a two-fold ambiguity. We can, however, select any of the two solutions without losing generality as discussed in Section 2.2.

For an initially pure $\overline{\mathrm{P}}^0$ state,

$$|\overline{\mathrm{P}}^0(t)\rangle = \frac{1}{\zeta} f_-(t)\,|\mathrm{P}^0\rangle + f_+(t)\,|\overline{\mathrm{P}}^0\rangle \tag{27}$$

$$= \frac{\sqrt{1+|\zeta|^2}}{2\,\zeta}\left(\,|\mathrm{P}_+\rangle\,e^{-\,i\,\lambda_+\,t} - |\mathrm{P}_-\rangle\,e^{-\,i\,\lambda_-\,t}\,\right) \tag{28}$$

describes the time evolution of the state.

It is common to introduce

$$\lambda_\pm \equiv m_\pm - \frac{i}{2}\Gamma_\pm$$

where

$$m_\pm = \Re\lambda_\pm = M \,\pm\, \Re\,(\,\Lambda_{12}\,\Lambda_{21}\,)^{1/2} \tag{29}$$

and

$$\Gamma_\pm = -2\,\Im\lambda_\pm = \Gamma \,\mp\, 2\,\Im\,(\,\Lambda_{12}\,\Lambda_{21}\,)^{1/2} \ . \tag{30}$$

While $\mathrm{P}_\pm$ have definite masses, $m_\pm$, and decay widths, $\Gamma_\pm$ (as seen from Equations 23 and 28), P^0 and $\overline{\mathrm{P}}^0$ do not and they oscillate into each other (see Equations 22 and 27).

2.2 CP Conserving Case

If V remains invariant under the CP transformation, from Equations 2, 13 and 14 it follows that

$$M_{12} = M_{21}e^{-i\,2\,\theta_{\mathrm{CP}}} = M_{12}^*e^{-i\,2\,\theta_{\mathrm{CP}}}$$

thus

$$\arg M_{12} = -\theta_{\mathrm{CP}} + n\pi,$$

and

$$\Gamma_{12} = \Gamma_{21}e^{-i\,2\,\theta_{\mathrm{CP}}} = \Gamma_{12}^*e^{-i\,2\,\theta_{\mathrm{CP}}}$$

thus

$$\arg \Gamma_{12} = -\theta_{\mathrm{CP}} + n'\pi,$$

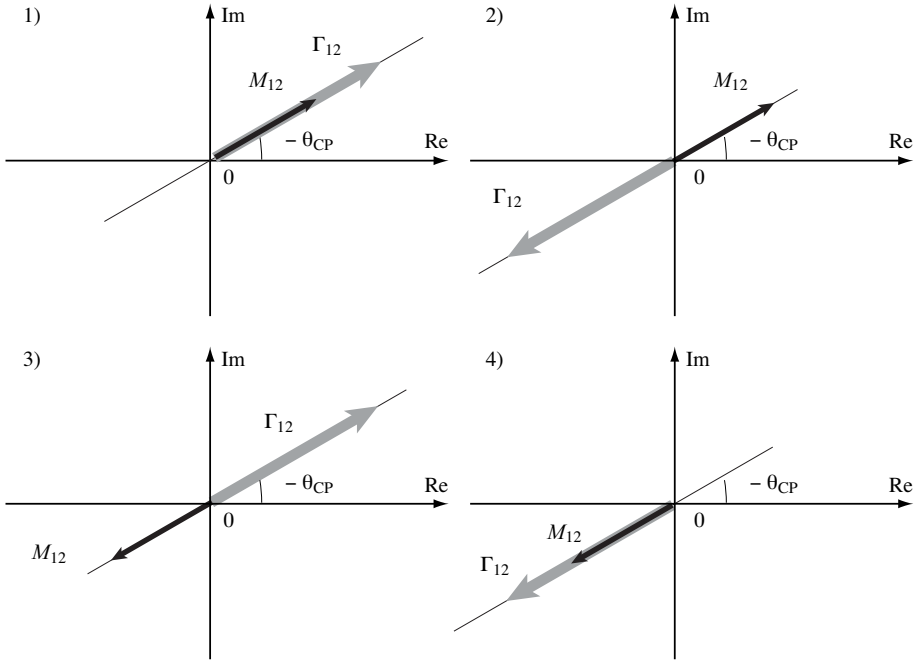

Figure 1: Relative phase relations for M_{12}, Γ_{12}, and CP transformation phase $\theta_{\rm CP}$ when CP is conserved: 1) $CP = +1$ state is heavier and decays faster, 2) $CP = +1$ state is heavier and decays slower, 3) $CP = +1$ state is lighter and decays faster, 4) $CP = +1$ state is lighter and decays slower.

where n and n' are arbitrary integer numbers.

For ζ, we have

$$\zeta = \sqrt{\frac{\Lambda_{21}}{\Lambda_{12}}} = e^{i\,(\theta_{\rm CP}+n''\pi)}$$

where n'' is 0 or 1 due to the two-fold ambiguity in the square-root operation of a complex number mentioned earlier. The two mass eigenstates $|{\rm P}_+\rangle$ and $|{\rm P}_-\rangle$ become CP eigenstates

$$CP|{\rm P}_\pm\rangle = \pm\,(-1)^{n''}|{\rm P}_\pm\rangle\ .$$

The masses and decay widths of $\rm P_\pm$ are derived from Equations 26, 29 and 30 as

$$m_\pm = M \pm (-1)^{n+n''}|M_{12}|$$

and

$$\Gamma_\pm = \Gamma \pm (-1)^{n'+n''}|\Gamma_{12}|\ .$$

By examining various combinations of n, n' and n'', we can show that the following four physical possibilities exist:

1. n=even, n'=even: $CP = +1$ state is heavier and decays faster,
2. n=even, n'=odd: $CP = +1$ state is heavier and decays slower,
3. n=odd, n'=even: $CP = +1$ state is lighter and decays faster,
4. n=odd, n'=odd: $CP = +1$ state is lighter and decays slower.

Figure 1 illustrates the phase relations in a pictorial way. The choice of n'' does not alter the conclusion and $n'' = 0$ can be adopted without any loss of generality. In this case, $|\mathrm{P}_+\rangle$ is the $CP = +1$ state and $|\mathrm{P}_-\rangle$ the $CP = -1$ state. If $n'' = 1$ would be adopted instead, $|\mathrm{P}_+\rangle$ would be the $CP = -1$ state and $|\mathrm{P}_-\rangle$ the $CP = +1$ state. This is equivalent to swapping the notations for P_+ and P_-. *We adopt $n'' = 0$ from now on.*

2.3 CP Violating Case

Let us consider the time dependent decay rate for the initial P^0 decaying into a CP eigenstate f, given by $|\langle f|V|\mathrm{P}^0(t)\rangle|^2$, and that for the initial $\overline{\mathrm{P}}^0$ decaying into f, given by $|\langle f|V|\overline{\mathrm{P}}^0(t)\rangle|^2$:

$$R_{\mathrm{f}}(t) \propto |f_+(t)|^2 + \left|\zeta\frac{\overline{A}_{\mathrm{f}}}{A_{\mathrm{f}}}\right|^2 |f_-(t)|^2 + 2\Re\left[\zeta\frac{\overline{A}_{\mathrm{f}}}{A_{\mathrm{f}}} f_+^*(t) f_-(t)\right] \tag{31}$$

$$\overline{R}_{\mathrm{f}}(t) \propto \left|\frac{\overline{A}_{\mathrm{f}}}{A_{\mathrm{f}}}\right|^2 |f_+(t)|^2 + \left|\frac{1}{\zeta}\right|^2 |f_-(t)|^2 + \frac{2}{|\zeta|^2}\Re\left[\zeta^*\frac{\overline{A}_{\mathrm{f}}^*}{A_{\mathrm{f}}^*} f_+^*(t) f_-(t)\right] \tag{32}$$

where the instantaneous decay amplitudes are denoted by $A_{\mathrm{f}} \equiv \langle \mathrm{f}|V|\mathrm{P}^0\rangle$ etc. and Equations 22 and 27 are used.

Since $R_{\mathrm{f}}(t)$ and $\overline{R}_{\mathrm{f}}(t)$ describe the decay rates of the CP-conjugated processes to each other, any difference between the two rates is a clear proof of CP violation. As seen from the first terms of Equations 31 and 32, CP violation is generated if $|A_{\mathrm{f}}| \neq |\overline{A}_{\mathrm{f}}|$. This is called **CP violation in the decay amplitudes**.

From the second terms of $R_{\mathrm{f}}(t)$ and $\overline{R}_{\mathrm{f}}(t)$, it can be seen that CP violation is generated if $|\zeta| \neq 1$ even if there is no CP violation in the decay amplitudes. From Equations 22 and 27, it is clear that the oscillation rate for $\mathrm{P}^0 \to \overline{\mathrm{P}}^0$ is different from that for $\overline{\mathrm{P}}^0 \to \mathrm{P}^0$ if $|\zeta| \neq 1$, thus this is called **CP violation in the oscillation**.

The third term can be expanded into

$$2\Re\left(\zeta\frac{\overline{A}_{\mathrm{f}}}{A_{\mathrm{f}}}\right)\Re\left[f_+^*(t) f_-(t)\right] - 2\Im\left(\zeta\frac{\overline{A}_{\mathrm{f}}}{A_{\mathrm{f}}}\right)\Im\left[f_+^*(t) f_-(t)\right]$$

for $R_{\rm f}(t)$ and

$$\frac{2}{|\zeta|^2}\Re\left(\zeta\frac{\overline{A}_{\rm f}}{A_{\rm f}}\right)\Re\left[f_+^*(t)f_-(t)\right]+\frac{2}{|\zeta|^2}\Im\left(\zeta\frac{\overline{A}_{\rm f}}{A_{\rm f}}\right)\Im\left[f_+^*(t)f_-(t)\right]$$

for $\overline{R}_{\rm f}(t)$. If CP violation in $\rm P^0$-$\overline{\rm P}^0$ oscillation is absent, the first terms are identical. Even in that case, if

$$\Im\left(\zeta\frac{\overline{A}_{\rm f}}{A_{\rm f}}\right)\neq 0$$

CP violation is still present. Since the process involves the decays of $\rm P^0$ ($\overline{\rm P}^0$) from the initial $\rm P^0$ ($\overline{\rm P}^0$) and decays of the $\overline{\rm P}^0$ ($\rm P^0$) oscillated from the initial $\rm P^0$ ($\overline{\rm P}^0$) into a common final state, it is referred to as **CP violation due to the interplay between decay and oscillation**.

If CP violation in $\rm P^0$-$\overline{\rm P}^0$ oscillation is small, i.e. $(|\zeta|-1)^2 \ll 1$, it follows from Equation 24 that

$$\frac{|\Im\left(M_{12}^*\Gamma_{12}\right)|}{4|M_{12}|^2+|\Gamma_{12}|^2}\ll 1$$

which can be due to

a) $|\sin(\varphi_\Gamma-\varphi_M)|\ll 1$

b) $|\Gamma_{12}/M_{12}|\ll 1$

c) $|M_{12}/\Gamma_{12}|\ll 1$

where $\varphi_\Gamma=\arg\Gamma_{12}$ and $\varphi_M=\arg M_{12}$.

As explained in the following section, condition a) applies in the case of the neutral kaon system. By introducing

$$\varphi_\Gamma-\varphi_M=N\,\pi-\Delta_{\Gamma/M} \tag{33}$$

where $|\Delta_{\Gamma/M}|\ll 1$ and N is an integer number, ζ can be approximated as

$$\begin{aligned}\zeta &\approx \left\{1-\frac{2|M_{12}||\Gamma_{12}|\Delta_{\Gamma/M}}{4|M_{12}|^2+|\Gamma_{12}|^2}\left[(-1)^{N+1}+i\frac{2|M_{12}|}{|\Gamma_{12}|}\right]\right\}e^{-i\,\varphi_\Gamma} \qquad (34)\\ m_\pm &= M\pm(-1)^N|M_{12}|\\ \Gamma_\pm &= \Gamma\pm|\Gamma_{12}|\end{aligned}$$

For the $\rm B_d$ and $\rm B_s$ meson systems, conditions a) and b) apply, and ζ can be approximated as

$$\begin{aligned}\zeta &\approx \left\{1+\Im\left(\frac{\Gamma_{12}}{M_{12}}\right)\right\}e^{-i\,\varphi_M} \qquad (35)\\ m_\pm &= M\pm|M_{12}|\\ \Gamma_\pm &= \Gamma\pm(-1)^N|\Gamma_{12}|\ .\end{aligned}$$

3 Neutral Kaon System

3.1 Adaptation of Formalism

Now we adapt the formalism developed above to the neutral kaon system. The two mass eigenstates are called $\mathrm{K_S}$ and $\mathrm{K_L}$ with corresponding masses and decay widths referred to as m_S, m_L, Γ_S and Γ_L respectively. More than 99% of the neutral kaon decays are into the two-pion final states ($\pi^+\pi^-$ and $\pi^0\pi^0$), which have $CP = +1$. The next largest (but very much smaller) decay modes are $\pi^+\pi^-\pi^0$, which is mainly $CP = -1$, and $\pi^0\pi^0\pi^0$, which is totally $CP = -1$. In the absence of CP violation only $\mathrm{K_S}$ can decay into the two-pion final states and $\mathrm{K_L}$ only into three-pion final states. This explains the observed pattern of $\Gamma_\mathrm{S} \gg \Gamma_\mathrm{L}$. It is also known that $m_\mathrm{S} < m_\mathrm{L}$. Furthermore, tiny CP violation effects are well established in the $\mathrm{K_L}$ decays. In conclusion, M_{12} and Γ_{12} are **almost antiparallel to each other** (but not exactly) and $N = 1$ in Equation 33.

From Equation 34, it follows that

$$\zeta = (1 - 2\epsilon)e^{-i\varphi_\Gamma} \tag{36}$$

where the small parameter ϵ is given by

$$\epsilon = \frac{|M_{12}||\Gamma_{12}|\sin(\varphi_\Gamma - \varphi_M)}{4|M_{12}|^2 + |\Gamma_{12}|^2}\left(1 + i\frac{2|M_{12}|}{|\Gamma_{12}|}\right) .$$

For Equation 25, $\mathrm{K_S}$ corresponds to $\mathrm{P_+}$ and $\mathrm{K_L}$ to $\mathrm{P_-}$ and we obtain

$$|\mathrm{K_S}\rangle = \frac{1}{\sqrt{2 - 4\Re\epsilon}}\left[|\mathrm{K^0}\rangle + (1 - 2\epsilon)e^{-i\varphi_\Gamma}|\overline{\mathrm{K}}^0\rangle\right] \tag{37}$$

$$|\mathrm{K_L}\rangle = \frac{1}{\sqrt{2 - 4\Re\epsilon}}\left[|\mathrm{K^0}\rangle - (1 - 2\epsilon)e^{-i\varphi_\Gamma}|\overline{\mathrm{K}}^0\rangle\right] . \tag{38}$$

From the measured lifetimes [16],

$$\tau_\mathrm{s} \equiv \frac{1}{\Gamma_\mathrm{S}} = (0.8935 \pm 0.0008) \times 10^{-10}\ \mathrm{s}$$

and

$$\tau_\mathrm{L} \equiv \frac{1}{\Gamma_\mathrm{L}} = (5.17 \pm 0.04) \times 10^{-8}\ \mathrm{s}$$

i.e.

$$\Delta\Gamma = \Gamma_\mathrm{S} - \Gamma_\mathrm{L} = (1.1173 \pm 0.0010) \times 10^{10}\ \mathrm{s}^{-1}$$

and the mass difference [16],

$$\Delta m \equiv m_\mathrm{L} - m_\mathrm{S} = (0.5303 \pm 0.0009) \times 10^{10}\ \hbar\mathrm{s}^{-1}$$

we obtain,

$$\frac{|M_{12}||\Gamma_{12}|}{4|M_{12}|^2+|\Gamma_{12}|^2} = 0.24966 \pm 0.00002$$

and

$$\frac{2|M_{12}|}{|\Gamma_{12}|} = 0.9492 \pm 0.0018 \ .$$

Since the lifetime of K_L is much longer than that of K_S, it is possible to produce a K_L beam. Therefore, many kaon experiments have been done using K_L beams.

3.2 CP Violation in Oscillations

The CPLEAR experiment observed CP violation in K^0-$\overline{K}^0$ oscillation by measuring the difference in the oscillation rates between $\overline{K}^0 \to K^0$ and $K^0 \to \overline{K}^0$. The initial neutral kaons were produced in $p\overline{p}$ annihilations: $p\overline{p} \to K^0K^-\pi^+$ and $\overline{K}^0K^+\pi^-$, where the initial flavour can be identified by the charge sign of the accompanying kaon. Semileptonic decays were used in order to determine the flavour at the moment of the decay. Since the K^0 contains an $\overline{s}$-quark (and $\overline{K}^0$ an s-quark), K^0 ($\overline{K}^0$) can decay only into $e^+\pi^-\nu$ ($e^-\pi^+\overline{\nu}$) instantaneously. Therefore, the initial K^0 ($\overline{K}^0$) can produce the final state $e^-\pi^+\overline{\nu}$ ($e^+\pi^-\nu$) only through the $K^0 \to \overline{K}^0$ ($\overline{K}^0 \to K^0$) oscillation. From the two measured time dependent decay rates, $R_{e^-}(t)$ and $\overline{R}_{e^+}(t)$, an asymmetry

$$A_T(t) = \frac{\overline{R}_{e^+}(t) - R_{e^-}(t)}{\overline{R}_{e^+}(t) + R_{e^-}(t)}$$

is constructed as shown in Figure 2. Using Equations 22, 27 and 36, it follows that

$$A_T(t) = \frac{1-|\zeta|^4}{1+|\zeta|^4} = 4\,\Re\epsilon$$

and from the measurement $A_T(t) = (6.6 \pm 1.6) \times 10^{-3}$ [17],

$$|\zeta| = 0.9967 \pm 0.0008 \neq 1$$

is obtained exhibiting a clear sign of CP violation and T violation in K^0-$\overline{K}^0$ oscillation.

The parameter $|\zeta|$ can also be measured from the semileptonic branching fractions of K_L by the lepton sign asymmetry: using Equations 38 and 36, we obtain [16, 18]

$$\begin{aligned}
\delta_\ell &\equiv \frac{B(K_L \to \ell^+\pi^-\nu) - B(K_L \to \ell^-\pi^+\overline{\nu})}{B(K_L \to \ell^+\pi^-\nu) + B(K_L \to \ell^-\pi^+\overline{\nu})} \\
&= \frac{1-|\zeta|^2}{1+|\zeta|^2} = 2\Re\epsilon \\
&= (3.307 \pm 0.064) \times 10^{-3}
\end{aligned}$$

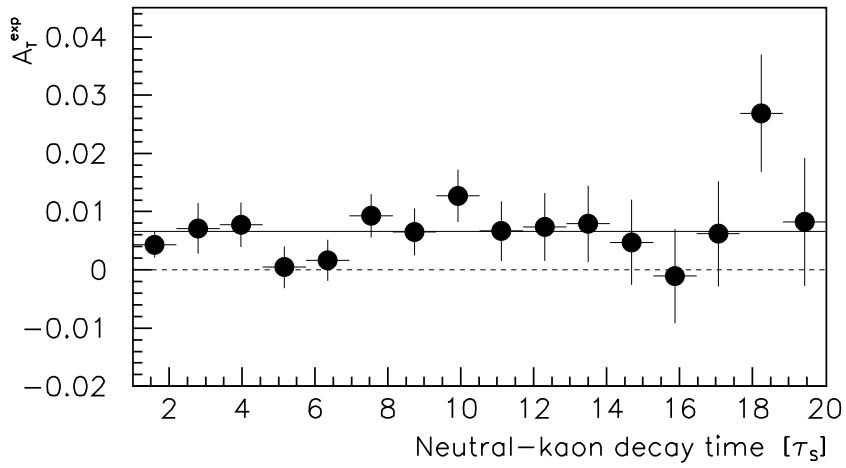

Figure 2: Measured rate asymmetry between the initial $\overline{\mathrm{K}}^0$ decaying into $\mathrm{e}^+\pi^-\nu$ and the initial K^0 decaying into $\mathrm{e}^-\pi^+\overline{\nu}$ as a function of the decay time in units of τ_S by the CPLEAR experiment [17]. The solid line is obtained by fitting a constant value.

where ℓ can be e or μ and B stands for a branching fraction.

Using all the measurements, we obtain

$$\Re\epsilon = (1.64 \pm 0.06) \times 10^{-3} \tag{39}$$

and

$$\arg\epsilon = \tan^{-1}\frac{2|M_{12}|}{|\Gamma_{12}|} = \tan^{-1}\frac{2\Delta m}{\Delta\Gamma} = (43.51 \pm 0.05)^\circ.$$

3.3 CP Violation due to Decays and Oscillations

Since the two-pion final state is a CP eigenstate with $CP = +1$, $\mathrm{K_L}$ decaying into $\pi^+\pi^-$ is a CP violating decay. This was indeed the first observed sign of CP violation. A commonly used CP violation parameter η_{+-} is defined as

$$\eta_{+-} \equiv \frac{\langle\pi^+\pi^-|V|\mathrm{K_L}\rangle}{\langle\pi^+\pi^-|V|\mathrm{K_S}\rangle} = \frac{1-\zeta\dfrac{\overline{A}_{+-}}{A_{+-}}}{1+\zeta\dfrac{\overline{A}_{+-}}{A_{+-}}} \tag{40}$$

where Equations 37, 38 are used and A_{+-} and $\overline{A}_{+-}$ denote the K^0 and $\overline{\mathrm{K}}^0 \to \pi^+\pi^-$ decay amplitudes respectively.

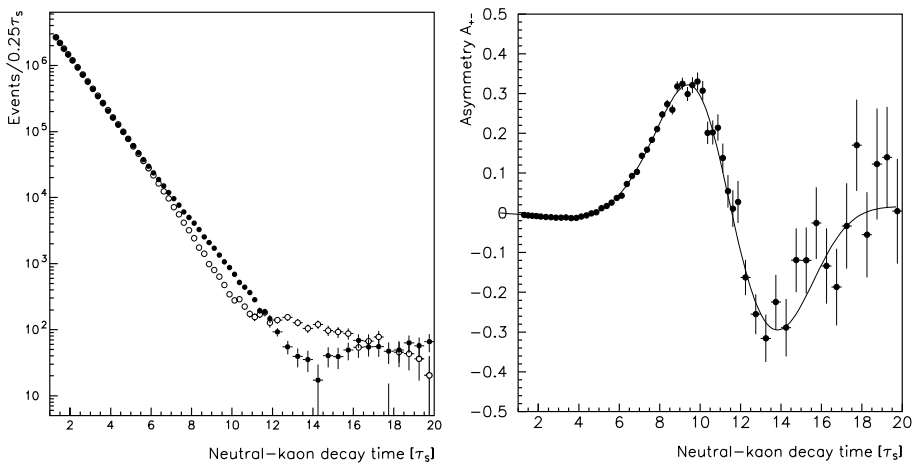

Figure 3: The time dependent rate distributions for the initial $\overline{\mathrm{K}}^0$ (solid circles) and K^0 (open circles) decaying into $\pi^+\pi^-$ as a function of the decay time in units of τ_S obtained by the CPLEAR experiment [19]. The rate asymmetry is also shown.

The parameter η_{+-} can be measured from the time dependent decay rates for the initial K^0 and $\overline{\mathrm{K}}^0$ into $\pi^+\pi^-$. From Equations 23 and 28, the two rates are given by

$$R_{+-}(t) \propto \frac{1}{2} e^{-\Gamma_\mathrm{S} t} + |\eta_{+-}|^2 e^{-\Gamma_\mathrm{L} t} + 2|\eta_{+-}| e^{-\bar{\Gamma} t} \cos(\Delta m\, t - \phi_{+-})$$

and

$$\overline{R}_{+-}(t) \propto \frac{1 + 4\Re\epsilon}{2} \left[e^{-\Gamma_\mathrm{S} t} + |\eta_{+-}|^2 e^{-\Gamma_\mathrm{L} t} - 2|\eta_{+-}| e^{-\bar{\Gamma} t} \cos(\Delta m\, t - \phi_{+-}) \right]$$

where ϕ_{+-} is the phase of η_{+-} and $\bar{\Gamma}$ is the $\mathrm{K_S}$-$\mathrm{K_L}$ average decay width. The second term is CP violating $\mathrm{K_L}$ decays and the third term is due to the interference between the $\mathrm{K_S}$ decay and CP violating $\mathrm{K_L}$ decay amplitudes. Figure 3 shows [19] the measured $R_{+-}(t)$ and $R_{+-}(t)$ together with the CP asymmetry defined as

$$A_{+-}(t) = \frac{\overline{R}_{+-}(t) - R_{+-}(t)}{\overline{R}_{+-}(t) + R_{+-}(t)}$$

where the interference term is well isolated. At around $t = 10\tau_\mathrm{S}$, the $\mathrm{K_S}$ decay rate is reduced to the level of the CP violating $\mathrm{K_L}$ decay rate, thus the asymmetry becomes very large.

This direct comparison between the two CP-conjugated processes provides another straightforward demonstration of CP violation in the neutral kaon system.

From the asymmetry, the value of η_{+-} is measured to be [19]

$$|\eta_{+-}| = (2.286 \pm 0.017) \times 10^{-3} \tag{41}$$

$$\phi_{+-} = (43.51 \pm 0.06)^{\circ} \tag{42}$$

which leads to

$$\Im\left(\zeta \frac{\overline{A}_{+-}}{A_{+-}}\right) = -(3.148 \pm 0.024) \times 10^{-3}$$

exhibiting that CP violation due to the interference between the decay and oscillation is present.

3.4 CP Violation in Decays

The two-pion final state can be in a total isospin state of $I = 0$ or $I = 2$. The $I = 1$ state is not allowed due to Bose statistics. Using the isospin decomposition, we can derive the K^0 and $\overline{\mathrm{K}}^0$ decay amplitudes to $\pi^+\pi^-$ to be

$$A_{+-} = \sqrt{\frac{2}{3}}\langle 2\pi(I=0)|V|\mathrm{K}^0\rangle + \sqrt{\frac{1}{3}}\langle 2\pi(I=2)|V|\mathrm{K}^0\rangle$$

and

$$\overline{A}_{+-} = \sqrt{\frac{2}{3}}\langle 2\pi(I=0)|V|\overline{\mathrm{K}}^0\rangle + \sqrt{\frac{1}{3}}\langle 2\pi(I=2)|V|\overline{\mathrm{K}}^0\rangle \ .$$

Using CPT symmetry and the S-matrix, the K^0 and $\overline{\mathrm{K}}^0$ decay amplitudes can be related and it follows that

$$\begin{aligned} A_{+-} &= \sqrt{\frac{2}{3}} a_0 e^{i\,\delta_0} + \sqrt{\frac{1}{3}} a_2 e^{i\,\delta_2} \\ \overline{A}_{+-} &= \sqrt{\frac{2}{3}} a_0^* e^{i\left(\delta_0 + \theta_{\mathrm{CP}} - \overline{\theta}_{\mathrm{T}}\right)} + \sqrt{\frac{1}{3}} a_2^* e^{i\left(\delta_2 + \theta_{\mathrm{CP}} - \overline{\theta}_{\mathrm{T}}\right)} \end{aligned}$$

where a_0 and a_2 are the K^0 decay amplitudes into $2\pi(I = 0)$ and $2\pi(I = 2)$ states due to the short-range weak interactions and δ_0 and δ_2 are the π-π scattering phase shifts for the $I = 0$ and $I = 2$ two-pion configuration at $\sqrt{s} = m_{\mathrm{K}}$ respectively. It is important to note that the two-pion scattering is totally dominated by elastic scattering at the energy scale of the kaon mass. Similarly for the $\pi^0\pi^0$ final state, we have

$$\begin{aligned} A_{00} &= -\sqrt{\frac{1}{3}} a_0 e^{i\,\delta_0} + \sqrt{\frac{2}{3}} a_2 e^{i\,\delta_2} \\ \overline{A}_{00} &= -\sqrt{\frac{1}{3}} a_0^* e^{i\left(\delta_0 + \theta_{\mathrm{CP}} - \overline{\theta}_{\mathrm{T}}\right)} + \sqrt{\frac{2}{3}} a_2^* e^{i\left(\delta_2 + \theta_{\mathrm{CP}} - \overline{\theta}_{\mathrm{T}}\right)} \ . \end{aligned}$$

As seen from the amplitudes, $B(\mathrm{K_S} \to \pi^0\pi^0)/B(\mathrm{K_S} \to \pi^+\pi^-)$ would be 0.5 if $a_2 = 0$. Since the measured ratio is ~ 0.46 [16], we can conclude that $|a_2/a_0| \ll 1$. It follows that

$$\frac{\overline{A}_{+-}}{A_{+-}} = (1 - 2\epsilon')\, e^{-i\left(2\varphi_0 + \overline{\theta}_{\mathrm{T}} - \theta_{\mathrm{CP}}\right)} \tag{43}$$

where the parameter ϵ' is given by

$$\epsilon' = \frac{1}{\sqrt{2}} \left|\frac{a_2}{a_0}\right| \sin(\varphi_2 - \varphi_0) e^{i(\pi/2 + \delta_2 - \delta_0)} \tag{44}$$

and $\varphi_{0,\,2} = \arg a_{0,\,2}$.

As seen from Equation 43, CP violation in the decay amplitude, $|A_{+-}| \neq |\overline{A}_{+-}|$, is present if $\Re\epsilon' \neq 0$. From Equation 44, this is possible only if

$$\sin(\varphi_2 - \varphi_0) \neq 0 \text{ and } \sin(\delta_2 - \delta_0) \neq 0 \ .$$

i.e. both the weak and strong phases have to be different for the $I = 0$ and $I = 2$ decay amplitudes. More generally, there must be two processes leading to the identical final state and both the strong and the weak phases must be different between the two processes in order to generate CP violation in the decay amplitudes. It should be noted that from the measured π-π scattering phase shift values, we have [20]

$$\arg \epsilon' = (43 \pm 6)^\circ \ .$$

Using Equations 36 and 43, it follows that

$$\begin{aligned} \zeta\frac{\overline{A}_{+-}}{A_{+-}} &= (1 - 2\epsilon - 2\epsilon')e^{-i\,(\varphi_\Gamma + 2\varphi_0 + \overline{\theta}_{\mathrm{T}} - \theta_{\mathrm{CP}})} \\ &\approx 1 - 2(\epsilon + \epsilon') - i\,(\varphi_\Gamma + 2\varphi_0 + \overline{\theta}_{\mathrm{T}} - \theta_{\mathrm{CP}}) \end{aligned}$$

where the approximation is made assuming that the phase difference between Γ_{12} and $A_0\overline{A}_0$ is small, which will be justified later. From Equation 40, η_{+-} can be derived to be

$$\eta_{+-} = \epsilon + i(\varphi_\Gamma + 2\varphi_0 + \overline{\theta}_{\mathrm{T}} - \theta_{\mathrm{CP}}) + \epsilon' \ . \tag{45}$$

Similarly the CP violation parameter for the $\pi^0\pi^0$ decay channel, η_{00}, is given by

$$\eta_{00} = \epsilon + i(\varphi_\Gamma + 2\varphi_0 + \overline{\theta}_{\mathrm{T}} - \theta_{\mathrm{CP}}) - 2\epsilon' \ .$$

Thus, we expect CP violation parameters to be different between the $\pi^+\pi^-$ and $\pi^0\pi^0$ decay modes if $\epsilon' \neq 0$.

Figure 4 shows $|\eta_{+-}/\eta_{00}|^2$ measured by four recent experiments, NA31 [21] and E731 [22] in 1993 and KTeV [23] and NA48 [24] in 2002, together with the averaged

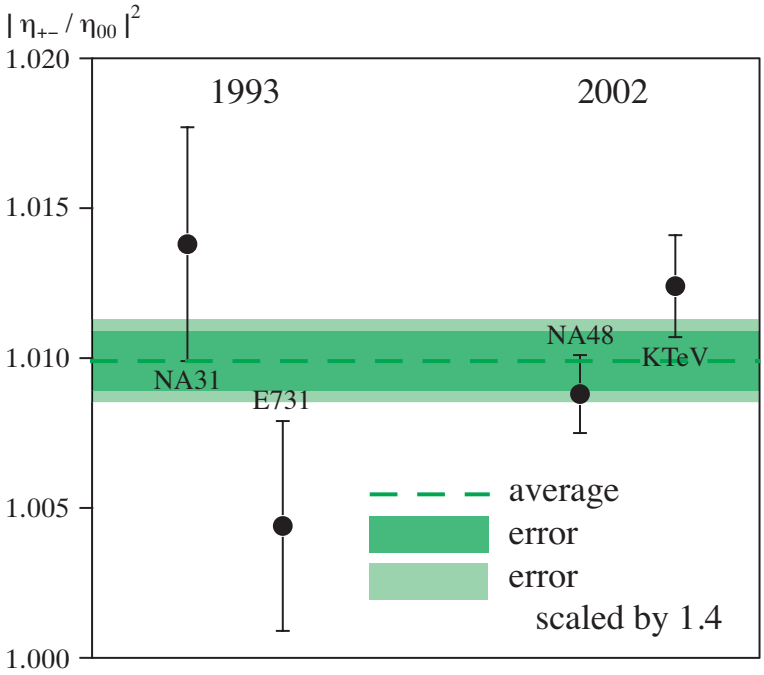

Figure 4: Most recent measurements of $|\eta_{+-}/\eta_{00}|^2$ together with the averaged value.

value. The averaged value is $|\eta_{+-}/\eta_{00}|^2 = 1.0099 \pm 0.0014$, where the error has been scaled by $\sqrt{\chi^2/3} = 1.4$, to account for the spread of central values of the measurements seen in the figure. It is clearly demonstrated that $|\eta_{+-}/\eta_{00}|^2 \neq 1$, i.e. CP violation in the decay amplitude is present in the neutral kaon system. As demonstrated in the next section, $(\varphi_\Gamma + 2\varphi_0 + \overline{\theta}_{\rm T} - \theta_{\rm CP})$ can be neglected and we obtain

$$\Re\left(\frac{\epsilon'}{\epsilon}\right) = \frac{1}{6}\left(\left|\frac{\eta_{+-}}{\eta_{00}}\right|^2 - 1\right) = (1.65 \pm 0.23) \times 10^{-3} \ . \tag{46}$$

From Equations 45, 39 and 46 and using the fact $\arg\epsilon \approx \arg\epsilon'$, $\Re\eta_{+-}$ is given by

$$\Re\eta_{+-} = \Re\epsilon + \Re\epsilon' \approx \Re\epsilon\left[1 + \Re\left(\frac{\epsilon'}{\epsilon}\right)\right] = (1.657 \pm 0.032) \times 10^{-3}$$

which agrees well with the measured value of $(1.658 \pm 0.012) \times 10^{-3}$ obtained from Equations 41 and 42.

3.5 Phase of Decay Matrix

As seen from Equation 14, evaluation of Γ_{12} involves the decay final states which are common to K^0 and $\overline{K}^0$, which are $2\pi(I=0)$, $2\pi(I=2)$, $3\pi(I=1)$, $3\pi(I=2)$ and $3\pi(I=3)$ states:

$$\Gamma_{12} \approx \sum_{I=0,2} A^*_{2\pi(I)} \overline{A}_{2\pi(I)} + \sum_{I=1,2,3} A^*_{3\pi(I)} \overline{A}_{3\pi(I)} \ .$$

The contribution from the decay amplitude to the $2\pi(I=2)$ state is suppressed by the $\Delta I = 1/2$ rule and the small measured value of ϵ'. The contribution from the three-pion decay amplitudes are suppressed by $\Gamma_{\rm L}/\Gamma_{\rm S}$ and the measured upper limits for the CP violation parameter for the $\pi^+\pi^-\pi^0$ and $\pi^0\pi^0\pi^0$ final states. In conclusion, the phase of Γ_{12} is essentially given by the phase of the A_0 amplitude, and it can be expressed as

$$\varphi_\Gamma \approx \arg A^*_0 \overline{A}_0 = -2\varphi_0 - \overline{\theta}_{\rm T} + \theta_{\rm CP}$$

so that

$$|\varphi_\Gamma + 2\varphi_0 + \overline{\theta}_{\rm T} - \theta_{\rm CP}| < O(10^{-5}) \ .$$

Thus $|\varphi_\Gamma + 2\varphi_0 + \overline{\theta}_{\rm T} - \theta_{\rm CP}| \ll |\epsilon|$, justifying the approximations made before.

3.6 The Standard Model

In the Standard Model, CP violation is naturally introduced by the 3×3 complex matrix [6], usually referred as Cabibbo-Kobayashi-Maskawa (CKM) quark mixing matrix [6, 7], V, expressed as

$$V = \begin{pmatrix} V_{\rm ud} & V_{\rm us} & V_{\rm ub} \\ V_{\rm cd} & V_{\rm cs} & V_{\rm cb} \\ V_{\rm td} & V_{\rm ts} & V_{\rm tb} \end{pmatrix} \ .$$

The charged current of the weak interaction is then proportional to

$$\overline{U}^i_{\rm L} \left(1 - \gamma_5\right) \gamma_\mu V_{ij} D^j_{\rm L} W^{+\mu}$$

where $U_{\rm L}$ and $D_{\rm L}$ are the left-handed quark operators for the charge 2/3 up-type and the charge $-1/3$ down-type quarks respectively: i.e.

$$U_{\rm L} = \begin{pmatrix} u_{\rm L} \\ c_{\rm L} \\ t_{\rm L} \end{pmatrix}, \text{ and } D_{\rm L} = \begin{pmatrix} d_{\rm L} \\ s_{\rm L} \\ b_{\rm L} \end{pmatrix} \ .$$

A unitary 3×3 matrix can be parameterized by four parameters. One possible choice [16] is to use the three angles and one phase, θ_{12}, θ_{23}, θ_{13} and δ respectively. Then the "standard" parameterization for the CKM matrix can be given by

$$V = R_{23} \times R_{13} \times R_{12}$$

where

$$R_{12} = \begin{pmatrix} c_{12} & s_{12} & 0 \\ -s_{12} & c_{12} & 0 \\ 0 & 0 & 1 \end{pmatrix}, R_{23} = \begin{pmatrix} 1 & 0 & 0 \\ 0 & c_{23} & s_{23} \\ 0 & -s_{23} & c_{23} \end{pmatrix}, R_{13} = \begin{pmatrix} c_{13} & 0 & s_{13}e^{-i\,\delta} \\ 0 & 1 & 0 \\ -s_{13}e^{i\,\delta} & 0 & c_{13} \end{pmatrix}$$

with $s_{ij} = \sin\theta_{ij}$ and $c_{ij} = \cos\theta_{ij}$.

A parametrization reflecting the observed pattern of the CKM matrix was first proposed by Wolfenstein [25]. First, we introduce the following transformation,

$$\lambda = \sin\theta_{12}, A = \frac{s_{23}}{s_{12}^2}, \rho = \frac{s_{13}\cos\delta}{s_{12}s_{23}}, \eta = \frac{s_{13}\sin\delta}{s_{12}s_{23}},$$

then expand the elements in powers of λ. By neglecting terms proportional to λ^n where $n > 5$, we obtain

$$V \approx \begin{pmatrix} 1-\lambda^2/2 & \lambda & A\lambda^3(\rho - i\,\eta) \\ -\lambda - i\,A^2\lambda^5\eta & 1-\lambda^2/2 & A\lambda^2 \\ A\lambda^3(1-\tilde{\rho} - i\,\tilde{\eta}) & -A\lambda^2 - i\,A\lambda^4\eta & 1 \end{pmatrix}, \tag{47}$$

where $\tilde{\rho}$ and $\tilde{\eta}$ are given by $\tilde{\rho} = \rho(1-\lambda^2/2)$ and $\tilde{\eta} = \eta(1-\lambda^2/2)$. From light hadron decays it is known [16] that

$$\lambda = 0.2229 \pm 0.0022 \tag{48}$$

justifying the approximation made to obtain equation 47. From B-meson decays, $|V_{\rm cb}|$ and $|V_{\rm ub}|$ are known to be $(40.6 \pm 0.8) \times 10^{-3}$ and $(3.63 \pm 0.32) \times 10^{-3}$ [27] respectively, leading to

$$A = 0.817 \pm 0.018 \tag{49}$$

$$\sqrt{\rho^2+\eta^2} = 0.40 \pm 0.04\ . \tag{50}$$

As seen from Equation 47, the first 2×2 sub-matrix is almost unitary, i.e.

$$V_{\rm ud}V_{\rm cd}^* + V_{\rm us}V_{\rm cs}^* = iA^2\lambda^5\eta \approx 0,\ V_{\rm ud}V_{\rm us}^* + V_{\rm cd}V_{\rm cs}^* = -iA^2\lambda^5\eta \approx 0$$

and

$$|V_{\rm ud}|^2 + |V_{\rm us}|^2 = 1 - \lambda^4/4 \approx 1,\ |V_{\rm cd}|^2 + |V_{\rm cs}|^2 = 1 - \lambda^4/4 \approx 1.$$

3.7 Flavour Oscillations in The Standard Model

In the framework of the Standard Model, the short-range contribution to K^0-$\overline{K}^0$ oscillation is obtained [26] from the box diagrams (Figure 5) to be

$$M_{12}^{\rm box} = -\frac{G_{\rm F}^2 f_{\rm K}^2 B_{\rm K} m_{\rm K} m_{\rm W}^2}{12\pi^2} \left[\eta_1 \sigma_{\rm c}^2 S(x_{\rm c}) + 2\eta_2 \sigma_{\rm c}\sigma_{\rm t} E(x_{\rm c}, x_{\rm t}) + \eta_3 \sigma_{\rm t}^2 S(x_{\rm t})\right]$$

where $G_{\rm F}$ is the Fermi constant, $f_{\rm K}$, $B_{\rm K}$ and $m_{\rm K}$ are the decay constant, B-parameter and mass of the K-meson respectively and $m_{\rm W}$ is the mass of the W-boson. The QCD correction factors are denoted by $\eta_1 = 1.38\pm0.20$, $\eta_2 = 0.57\pm0.01$ and $\eta_3 = 0.47\pm0.04$ and S and E are known functions of the mass ratios, $x_{\rm i} = m_{\rm i}^2/m_{\rm W}^2$ for top (i=t) and charm (i=c). Note that

$$S(x_{\rm c}) \approx 2.4 \times 10^{-4},\ S(x_{\rm t}) \approx 2.6,\ E(x_{\rm c},\ x_{\rm c}) \approx 2.2 \times 10^{-3} \tag{51}$$

for $m_{\rm c} = 1.25$ GeV/c^2, $m_{\rm t} = 174$ GeV/c^2 and $m_{\rm W} = 80$ GeV/c^2. The parameters $\sigma_{\rm c}$ and $\sigma_{\rm t}$ are the combination of the elements of the CKM-matrix as $\sigma_{\rm c} = V_{\rm cs}{V_{\rm cd}}^*$ and $\sigma_{\rm t} = V_{\rm ts}{V_{\rm td}}^*$. The B-parameter takes in account the difference between $\langle 0|V|{\rm K}^{\pm}\rangle$ and $\langle f|V|{\rm K}^0\rangle$ where $\langle 0|$ is the hadronic vacuum state and $\langle f|$ is the common quark states between K^0 and $\overline{K}^0$. The theoretical evaluations for this value vary between 0.5 and 1.

In addition to $M_{12}^{\rm box}$, there are large contributions from long-range interactions $M_{12}^{\rm LR}$, which are difficult to evaluate. Therefore, theoretical predication for $M_{12} = M_{12}^{\rm box} + M_{12}^{\rm LR}$ cannot be given. The long-range interaction involves only the light flavours and its contribution to M_{12} is real in the CKM phase convention; the imaginary part of M_{12} is generated only by the box diagram. Therefore we can derive

$$\sin(\varphi_M) = \frac{\Im M_{12}}{|M_{12}|} = \frac{2\,\Im M_{12}^{\rm box}}{\Delta m}\ .$$

In the CKM phase convention, Γ_{12} can be approximated as real. Therefore, it follows that

$$\Re\epsilon = -\frac{\Im M_{12}^{\rm box}}{2\,\Delta m}\ .$$

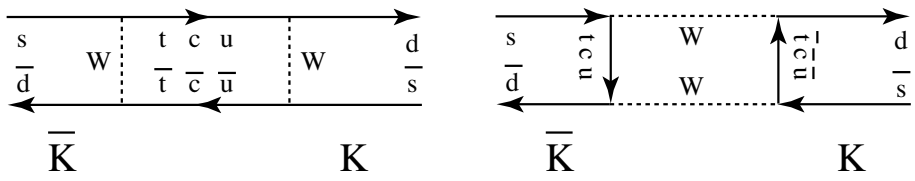

Figure 5: The box diagrams contributing to K^0-$\overline{K}^0$ oscillations.

Although there are considerable uncertainties to evaluate numerically this expression, the currently allowed range of the Wolfenstein parameters, λ, A, ρ and η given by Equations 48, 49 and 50 determines a value of $\Re\epsilon$ consistent with the experimentally measured value.

3.8 CP Violation in Decay Amplitudes

Prediction of ϵ' requires an accurate evaluation of the phase difference between a_0 and a_2. For the a_0 amplitudes, the tree, the gluonic penguin and the electroweak penguin diagrams contribute. Only the tree and electroweak penguin diagrams make contributions to the a_2 decay amplitude. All the penguin diagrams are shown in Figure 6. Not only the short range interactions, but also the hadronic matrix elements with long range interactions have to be evaluated in the calculations. This makes the numerical determination of ϵ' very difficult. The measured value of $\Re(\epsilon'/\epsilon)$ given in Equation 46 is well within the range of various theoretical predictions from -1.3×10^{-3} to 6.4×10^{-3} with the currently allowed range of λ, A, ρ and η. Note the large uncertainties in the predictions.

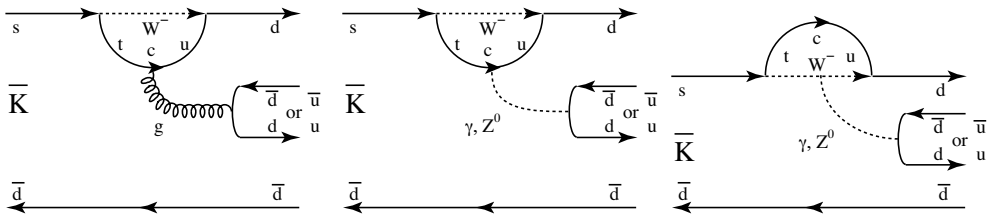

Figure 6: Gluonic and electromagnetic penguins contributing to the $\overline{\mathrm{K}}^0 \to 2\pi$ decays.

3.9 CP Violation in Rare Decays

Experimental detection of $\mathrm{K_L} \to \pi^0\nu\overline{\nu}$ is clearly very challenging. The final state is a CP eigenstate with $CP = +1$. Therefore, observation of this decay is a sign of CP violation. In the Standard Model, the decay is generated by penguin diagrams or box diagrams as shown in Figure 7.

Since the final state consists of only one hadron, long range strong interactions do not play a role and the decay amplitudes can be denoted as

$$\begin{aligned} \langle \pi^0\nu\overline{\nu}|V|\mathrm{K}^0\rangle &= a_{\pi^0\nu\overline{\nu}} \\ \langle \pi^0\nu\overline{\nu}|V|\overline{\mathrm{K}}^0\rangle &= a^*_{\pi^0\nu\overline{\nu}}\, e^{i\left(\theta_{\mathrm{CP}} - \overline{\theta}_{\mathrm{T}}\right)} \ . \end{aligned}$$

Unlike for the $K^0 \to 2\pi$ decays, $\phi_{\pi^0\nu\overline{\nu}} = \arg a_{\pi^0\nu\overline{\nu}}$ could be very different from ϕ_0, so that we could have the situation

$$\left|\sin\left(\phi_\Gamma + 2\,\phi_{\pi^0\nu\overline{\nu}} + \theta_{\rm CP} - \overline{\theta}_{\rm T}\right)\right| = \left|\sin\left(2\,\phi_{\pi^0\nu\overline{\nu}} - 2\phi_0\right)\right| \gg |\epsilon| \ .$$

The K_L decay amplitude then becomes

$$\begin{aligned}\langle\pi^0\nu\overline{\nu}|V|K_L\rangle &= \frac{a_{\pi^0\nu\overline{\nu}}}{\sqrt{2}}\left[1-(1-2\epsilon)e^{-i\,(2\,\phi_{\pi^0\nu\overline{\nu}}-2\phi_0)}\right] \\ &\approx \sqrt{2}\,i\,|a_{\pi^0\nu\overline{\nu}}|\sin(\phi_{\pi^0\nu\overline{\nu}}-\phi_0)\ .\end{aligned}$$

Using isospin symmetry, the hadronic matrix element of the $K^0 \to \pi^0\nu\overline{\nu}$ decay amplitude and that of the $K^+ \to \pi^0 e^+\nu$ decay amplitude can be related as

$$\langle\pi^0|V|K^0\rangle = \langle\pi^0|V|K^+\rangle\ .$$

This allows us to express the branching fraction for $K_L \to \pi^0\nu\overline{\nu}$ using the branching fraction for $K^+ \to \pi^0 e^+\nu$ as [26]

$$\begin{aligned}B(K_L\to\pi^0\nu\overline{\nu}) &= \frac{|\langle\pi^0\nu\overline{\nu}|V|K_L\rangle|^2}{\Gamma_L} \\ &= B(K^+\to\pi^0e^+\nu)\frac{\tau_L}{\tau_+}\frac{3\,\alpha^2\left[\Im(V_{ts}^*V_{td})X(x_t)\right]^2}{|V_{us}|^2 2\pi^2\sin^4\Theta_W} \\ &= B(K^+\to\pi^0e^+\nu)\frac{\tau_L}{\tau_+}\frac{3\,\alpha^2\left[X(x_t)\right]^2}{2\pi^2\sin^4\Theta_W}A^4\lambda^8(1-\lambda^2/2)^2\eta^2 \\ &\approx 3\times10^{-11}\end{aligned}$$

where X is a known function of $x_t = (m_t/m_W)^2$ and Θ_W is the weak mixing angle. Since the hadronic matrix element is taken from the data, the theoretical uncertainties in this determination is very small. Also the imaginary part of the amplitude is

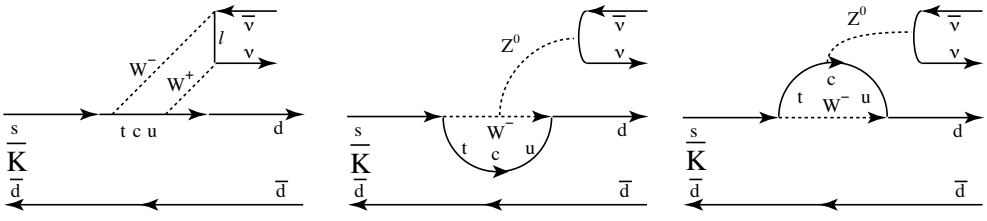

Figure 7: The box and penguin diagrams generating $\overline{K}^0 \to \pi^0\nu\overline{\nu}$ decays.

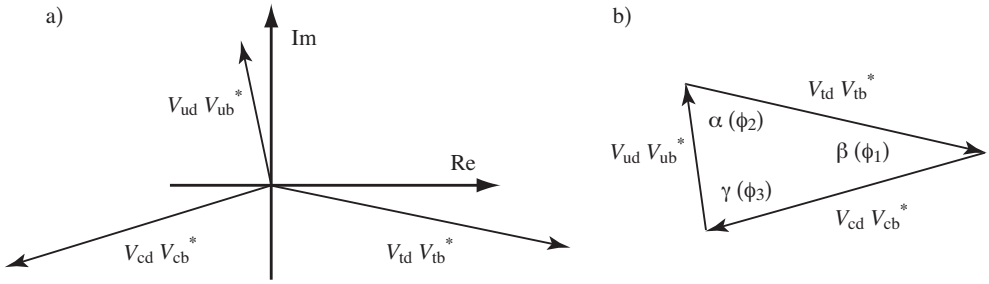

Figure 8: a) One of the unitarity conditions of the CKM matrix, $V_{\rm ud}V_{\rm ub}^* + V_{\rm cd}V_{\rm cb}^* + V_{\rm td}V_{\rm tb}^* = 0$ drawn in the complex plane. b) Elements transported so that a triangle can be formed.

dominated by the short range interactions which can be reliably calculated. Therefore, the theoretical prediction can be considered to be clean.

It is interesting to note that the CP violation parameter

$$\eta_{\pi^0\nu\overline{\nu}} \equiv \frac{\langle \pi^0\nu\overline{\nu}|V|{\rm K_L}\rangle}{\langle \pi^0\nu\overline{\nu}|V|{\rm K_S}\rangle} = i\tan(\phi_{\pi^0\nu\overline{\nu}} - \phi_0)$$

as defined in the 2π case, has $|\eta_{\pi^0\nu\overline{\nu}}| \gg |\epsilon|$, although both final states have $CP = +1$.

The current experimental upper limit for this branching fraction is 5.9×10^{-7} with 90% confidence by the KTeV experiment [28], which is still far from the expected number. However, an experiment is planned at BNL [1] with a sensitivity which should allow to observe this decay in the near future.

4 Neutral B-meson System

4.1 The Standard Model Description

4.1.1 Some CKM Matrix Elements

The matrix V is unitary, i.e. $V^\dagger V = 1$. One of the unitarity relations relevant for the B-meson systems

$$V_{\rm ud}V_{\rm ub}^* + V_{\rm cd}V_{\rm cb}^* + V_{\rm td}V_{\rm tb}^* = 0 \tag{52}$$

is illustrated in Figure 8-a in the complex plane. The unitarity condition can be illustrated easily by transporting $V_{\rm cd}V_{\rm cb}^*$ and $V_{\rm td}V_{\rm tb}^*$ so that a closed triangle is formed,

[1] KOPIO BNL-AGS-E926

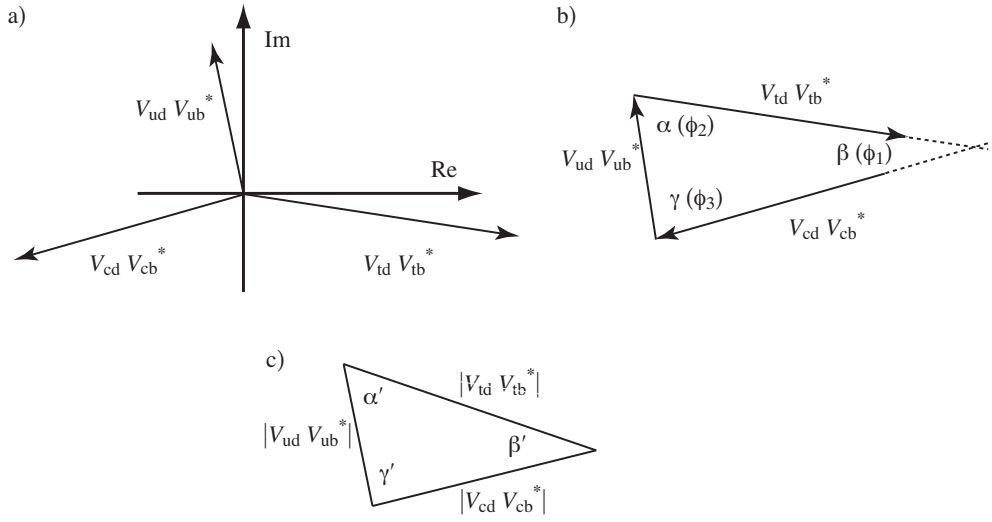

Figure 9: a) and b), are similar to Figure 8, however unitarity is violated. In c) a closed triangle is formed using the three sides.

as shown in Figure 8-b. Three angles of the triangle, α, β and γ (also known as ϕ_2, ϕ_1 and ϕ_3 respectively) can be defined as

$$\alpha = \tan^{-1}\frac{-V_{\rm td}V_{\rm tb}^*}{V_{\rm ud}V_{\rm ub}^*},\ \beta = \pi - \tan^{-1}\frac{V_{\rm td}V_{\rm tb}^*}{V_{\rm cd}V_{\rm cb}^*},\ \gamma = \tan^{-1}\frac{-V_{\rm ud}V_{\rm ub}^*}{V_{\rm cd}V_{\rm cb}^*}\ . \qquad (53)$$

It should be noted that a redefinition of the quark phases results in a rotation of the triangle while the three angles, α, β and γ remain invariant.

Violation of the unitarity condition given by Equation 52 is expressed in a graphical form in Figure 9-a and -b, where the three sides given by $V_{\rm ud}V_{\rm ub}^*$, $V_{\rm cd}V_{\rm cb}^*$ and $V_{\rm td}V_{\rm tb}^*$ do not form a closed triangle. Note that α, β and γ defined as Equations 53 still fulfill

$$\alpha + \beta + \gamma = \pi\ .$$

If one forms the closed triangle from the length of the three sides, $|V_{\rm ud}V_{\rm ub}^*|$, $|V_{\rm cd}V_{\rm cb}^*|$ and $|V_{\rm td}V_{\rm tb}^*|$, the three angles of this triangle, α', β' and γ' defined as in Figure 9-c, are not identical to α, β and γ. Therefore, a test of the unitarity can be made by comparing the angles defined by the length of the three sides and α, β or γ measured by CP violation as explained later.

With the parametrization given in Equation 47, the imaginary part of $V_{\rm cd}$ becomes negligible in the unitarity relation given by Equation 52. The phases of the elements

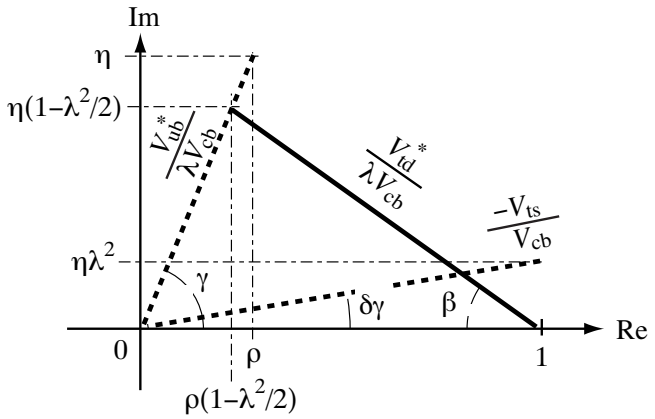

Figure 10: Three elements of the CKM matrix, $V_{\rm td}$, $V_{\rm ub}$, and $V_{\rm ts}$ and the definitions of β, γ and $\delta\gamma$.

those appear in the equation are given by

$$\arg V_{\rm td} = -\beta,\ \ \arg V_{\rm ub} = -\gamma,\ \ \arg V_{\rm ud} = \arg V_{\rm cb} = \arg V_{\rm tb} = 0 \text{ and } \arg V_{\rm cd} = \pi.$$

The imaginary part of $V_{\rm ts}$ cannot be ignored and

$$\arg V_{\rm ts} = \delta\gamma + \pi$$

where β, γ and and $\delta\gamma$ are determined by ρ, η and λ as

$$\beta = \tan^{-1}\frac{\eta}{1-\rho},\ \gamma = \tan^{-1}\frac{\eta}{\rho},\ \delta\gamma = \tan^{-1}\lambda^2\eta\ .$$

Figure 10 shows the angles in the ρ-η plane. Note that β and γ are also referred to as ϕ_1 and ϕ_3 respectively. Clearly $\delta\gamma$ is very small, ~ 0.02.

4.1.2 Oscillation Amplitude

In the Standard Model, B-$\overline{\rm B}$ oscillation is totally governed by the short range interactions, i.e. the box diagrams. Furthermore, only the top quark plays a role in the box diagram due to the large top quark mass (see Equation 51) and the structure of the CKM matrix;

$$\frac{\Re(V_{\rm td}^* V_{\rm tb})}{\Re(V_{\rm cd}^* V_{\rm cb})} = (\tilde{\rho} - 1) \approx 1,\ \ \frac{\Im(V_{\rm td}^* V_{\rm tb})}{\Im(V_{\rm cd}^* V_{\rm cb})} \approx \frac{1}{\lambda^2} \gg 1$$

as seen from Equation 47.

Therefore, the off-diagonal element of the mass matrix, M_{12} is given by [26]

$$M_{12} = -\frac{G_{\rm F}^2 f_{\rm B_d}^2 B_{\rm B_d} m_{\rm B_d} m_{\rm W}^2}{12\pi^2} \eta_{\rm B_d} S(x_{\rm t}) (V_{\rm td}^* V_{\rm tb})^2 \quad \text{for } {\rm B_d} \tag{54}$$

where $f_{\rm B_d}$, $B_{\rm B_d}$ and $m_{\rm B_d}$ are the decay constant, B-parameter and the mass of the $\rm B_d$ meson.

Similarly for the $\rm B_s$ meson, we obtain

$$M_{12} = -\frac{G_{\rm F}^2 f_{\rm B_s}^2 B_{\rm B_s} m_{\rm B_s} m_{\rm W}^2}{12\pi^2} \eta_{\rm B_s} S(x_{\rm t}) (V_{\rm ts}^* V_{\rm tb})^2 \quad \text{for } {\rm B_s}$$

where $f_{\rm B_s}$, $B_{\rm B_s}$ and $m_{\rm B_s}$ are the decay constant, B-parameter and the mass of the $\rm B_s$ meson.

The phase of M_{12} is then given by

$$\arg M_{12} = \begin{cases} \arg(V_{\rm td}^* V_{\rm tb})^2 + \pi = 2\beta + \pi & \text{for } {\rm B_d} \\ \arg(V_{\rm ts}^* V_{\rm tb})^2 + \pi = -2\delta\gamma + \pi & \text{for } {\rm B_s}. \end{cases}$$

The parameter Γ_{12} can also be determined by taking the absorptive part of the box diagrams with charm and up quarks in the loops. For both $\rm B_d$ and $\rm B_s$, we can derive

$$\left|\frac{\Gamma_{12}}{M_{12}}\right| \approx \frac{3\pi m_{\rm b}^2}{2 m_{\rm W}^2 S(x_{\rm t})} \approx 5 \times 10^{-3} \qquad \text{for } {\rm B_d} \text{ and } {\rm B_s} \tag{55}$$

for $m_{\rm b} = 4.25$ GeV/c^2, $m_{\rm W} = 80$ GeV/c^2 and $m_{\rm t} = 174$ GeV/c^2.

The phase difference between M_{12} and Γ_{12} is given by

$$\arg M_{12} - \arg \Gamma_{12} = \pi + \frac{8}{3}\left(\frac{m_{\rm c}}{m_{\rm b}}\right)^2 \eta \times \begin{cases} \dfrac{1}{(1-\rho)^2 + \eta^2} & : {\rm B_d} \\ \lambda^2 & : {\rm B_s} \end{cases} \tag{56}$$

i.e. $\sin(\arg M_{12} - \arg \Gamma_{12})$ is small for $\rm B_d$ and very small for $\rm B_s$. Note that M_{12} and Γ_{12} are antiparallel.

We can now adopt the approximations given by Equations 35 with $N = 1$ and derive

$$\zeta \approx \left[1 - \frac{1}{2}\,\Im\left(\frac{\Gamma_{12}}{M_{12}}\right)\right] e^{-i\,\varphi_M} \tag{57}$$

where $\varphi_M = \arg M_{12}$ as before. Seen from Equation 55 and 56, the approximation $|\zeta| \approx 1$ is accurate to 10^{-3} or better; i.e. CP violation in the oscillation is small for $\rm B_d$ and very small for $\rm B_s$.

By referring to the mass eigenstate with larger mass as B_h (B-heavy) and the other B_l (B-light) with their masses and decay width, it follows that:

$$m_h = M + |M_{12}|,\ \Gamma_h = \Gamma - |\Gamma_{12}|$$

and

$$m_l = M - |M_{12}|,\ \Gamma_l = \Gamma + |\Gamma_{12}|$$

respectively, and B_h (B_l) corresponds to P_+ (P_-) defined in Equation 25.

The mass and decay width differences between B_h and B_l, Δm and $\Delta\Gamma$ respectively, are defined as positive:

$$\Delta m = m_h - m_l,\ \Delta\Gamma = \Gamma_l - \Gamma_h\ .$$

Using the measured values of $\Delta m = (0.489 \pm 0.008) \times 10^{12}\ \hbar s^{-1}$ and the average lifetime $\tau = 1/\bar{\Gamma} = (1.542 \pm 0.016) \times 10^{-12}$ s for the B_d mesons [16], where $\bar{\Gamma}$ is the averaged decay width, it follows that

$$\frac{\Delta\Gamma}{\bar{\Gamma}} \approx 4 \times 10^{-3} \qquad \text{for } B_d$$

and $\Delta\Gamma$ can be neglected in the decay time distribution for the B_d system. For the B_s mesons, only the lower limit of Δm has been measured to be $13.1 \times 10^{12}\ \hbar\ s^{-1}$ with 95% confidence level [16]. Using the measured lifetime $(1.461 \pm 0.057) \times 10^{-12}$ s [16], it follows that

$$\frac{\Delta\Gamma}{\bar{\Gamma}} > 0.08 \qquad \text{for } B_s.$$

The effect of $\Delta\Gamma$ can no longer be neglected in the decay time distributions.

The small decay width differences of the B_d and B_s systems do not allow to separate one mass-eigenstate from the other, which can be done for the kaon system by creating a K_L beam. Therefore, CP violation cannot be established by just observing the decays as in the case of $K_L \to 2\pi$. We either have to compare the decay rates of the initial B^0 and initial $\overline{B}^0$ states or measure the time dependent decay rates of at least one of the two cases, i.e. either initial B^0 or $\overline{B}^0$.

The mass difference Δm_d is experimentally measured as the frequency of the B^0-$\overline{B}^0$ oscillation. From the known structure of the CKM matrix, we have $|V_{tb}| = 1$ with very high accuracy. Using $\Delta m = 2|M_{12}|$ and Equation 54, $|V_{td}|$ can be obtained from Δm_d. From Equation 47, it follows that

$$\sqrt{(1-\tilde{\rho})^2 + \tilde{\eta}^2} = \frac{|V_{td}|}{\lambda^3 A}\ . \tag{58}$$

The current measurements on Δm_d [16] leads to

$$\sqrt{(1-\tilde{\rho})^2 + \tilde{\eta}^2} = 0.86 \pm 0.17 \tag{59}$$

The error on $|V_{\rm td}|$ is totally dominated by the theoretical uncertainties on $f_{\rm B}\sqrt{B_{\rm d}}$.

Once $\Delta m_{\rm s}$ is measured,

$$\sqrt{(1-\tilde{\rho})^2+\tilde{\eta}^2} = \frac{|V_{\rm td}|}{\lambda|V_{\rm ts}|} = \frac{\sqrt{\Delta m_{\rm d}}}{\lambda\sqrt{\Delta m_{\rm s}}} \times \frac{\sqrt{m_{\rm B_s}\eta_{\rm B_s}}}{\sqrt{m_{\rm B_d}\eta_{\rm B_d}}} \times \frac{\sqrt{B_{\rm B_s}}f_{\rm B_s}}{\sqrt{B_{\rm B_d}}f_{\rm B_d}} \tag{60}$$

can be used instead of Equation 58, where the assumption $|V_{\rm tb}| = 1$ is no longer necessary. While the theoretical uncertainty in $f_B\sqrt{B}$ is quite considerable, the ratio between them for the $\rm B_s^0$ and $\rm B^0$ mesons is theoretically much better understood. Therefore, Equation 60 will have significantly smaller error than Equation 58. However, the frequency of the $\rm B_s^0$-$\overline{\rm B}_s^0$ oscillation is expected to be $> 1/\lambda^2 = 20$ times larger than that of the $\rm B^0$-$\overline{\rm B}^0$ oscillation and we may still have to wait for some time before it is measured.

Similar to the kaon system, CP violation (and T violation) in the oscillation can be measured from the time-dependent rate asymmetry between the initial $\overline{\rm B}^0$ decaying into semileptonic final states with $\rm e^+$ or μ^+, $\overline{R}_+(t)$ and the initial $\rm B^0$ decaying into semileptonic final states with $\rm e^-$ or μ^-, $R_-(t)$. The asymmetry is given by

$$\frac{\overline{R}_+(t)-R_-(t)}{\overline{R}_+(t)+R_-(t)} = \frac{1-|\zeta|^4}{1+|\zeta|^4} \approx O(10^{-3}) \text{ for } \rm B_d \text{ and } \ll O(10^{-3}) \text{ for } \rm B_s.$$

Experimentally, $1-|\zeta|^2 = 0.000 \pm 0.008$ for $\rm B_d$ [16].

From now on, we assume

$$\zeta = e^{-i\,\varphi_M}$$

for both $\rm B_d$ and $\rm B_s$ and $\Delta\Gamma = 0$ for $\rm B_d$.

In summary, the two mass eigenstates are given by

$$\begin{aligned} |{\rm B_h}\rangle &= \frac{1}{\sqrt{2}}\left[|{\rm B}\rangle + e^{-i\,\varphi_M}|\overline{\rm B}\rangle\right] \\ |{\rm B_l}\rangle &= \frac{1}{\sqrt{2}}\left[|{\rm B}\rangle - e^{-i\,\varphi_M}|\overline{\rm B}\rangle\right] \end{aligned}$$

and

$$m_{\rm h} = m_0 + |M_{12}|,\ m_{\rm l} = m_0 - |M_{12}|,\ \Delta m = m_{\rm h} - m_{\rm l}$$

for $\rm B_d$ and $\rm B_s$. For the decay width, we have

$$\begin{array}{ll} \Gamma_{\rm l} = \Gamma_{\rm h} & \text{for } \rm B_d \\ \Gamma_{\rm l} = \Gamma_0 + |\Gamma_{12}|,\ \Gamma_{\rm h} = \Gamma_0 - |\Gamma_{12}|,\ \Delta\Gamma = \Gamma_{\rm l} - \Gamma_{\rm h} & \text{for } \rm B_s \end{array}$$

4.1.3 Time Dependent Decay Rates

Since $\Delta\Gamma$ is small in the B meson system, it is more convenient to derive the time dependent decay rate from the particle-antiparticle base rather than the mass eigenstate base. Using, Equations 22 and 27 the time dependent decay rates for the final state f can be derived as

$$\begin{aligned} R_{\rm f}(t) &\propto \frac{|A_{\rm f}|^2}{2} e^{-\bar{\Gamma}\,t}\,[I_+(t) + I_-(t)] \\ \overline{R}_{\rm f}(t) &\propto \frac{|A_{\rm f}|^2}{2|\zeta|^2} e^{-\bar{\Gamma}\,t}\,[I_+(t) - I_-(t)] \end{aligned}$$

where $\bar{\Gamma}$ is the averaged decay time, $\bar{\Gamma} = (\Gamma_+ + \Gamma_-)/2$, and $A_{\rm f}$ is the instantaneous decay amplitude for the B^0 or $\mathrm{B}^0_{\rm s} \to \mathrm{f}$ decays. The two time dependent functions, $I_+(t)$ and $I_-(t)$, are given by

$$\begin{aligned} I_+(t) &= (1 + |L_{\rm f}|^2)\,\cosh\frac{\Delta\Gamma}{2}\,t + 2\Re L_{\rm f}\,\sinh\frac{\Delta\Gamma}{2}\,t \\ I_-(t) &= (1 - |L_{\rm f}|^2)\cos\Delta m\,t + 2\Im L_{\rm f}\,\sin\Delta m\,t\ . \end{aligned}$$

The parameter $L_{\rm f}$ is given by

$$L_{\rm f} = \zeta\frac{\overline{A}_{\rm f}}{A_{\rm f}}$$

where $\overline{A}_{\rm f}$ is the instantaneous decay amplitude for the $\overline{\mathrm{B}}^0$ or $\overline{\mathrm{B}}^0_{\rm s} \to \mathrm{f}$ decays.

The time dependent decay rate for the CP-conjugated final states $\mathrm{f}^{\rm CP}$ are derived to be

$$\begin{aligned} \overline{R}_{\rm fCP}(t) &\propto \frac{|\overline{A}_{\rm fCP}|^2}{2} e^{-\overline{\Gamma}\,t}\left[\overline{I}_+^{\rm CP}(t) + \overline{I}_-^{\rm CP}(t)\right] \\ R_{\rm fCP}(t) &\propto \frac{|\overline{A}_{\rm fCP}|^2|\zeta|^2}{2} e^{-\overline{\Gamma}\,t}\left[\overline{I}_+^{\rm CP}(t) - \overline{I}_-^{\rm CP}(t)\right] \end{aligned}$$

where $\overline{A}_{\rm fCP}$ is the instantaneous decay amplitude for the $\overline{\mathrm{B}}^0$ or $\overline{\mathrm{B}}^0_{\rm s} \to \mathrm{f}^{\rm CP}$ decays. Two time dependent decay rates, $\overline{I}_+^{\rm CP}(t)$ and $\overline{I}_-^{\rm CP}(t)$ are given by

$$\begin{aligned} \overline{I}_+^{\rm CP}(t) &= (1 + |L_{\rm f}^{\rm CP}|^2)\,\cosh\frac{\Delta\Gamma}{2}\,t + 2\Re L_{\rm f}^{\rm CP}\,\sinh\frac{\Delta\Gamma}{2}\,t \\ \overline{I}_-^{\rm CP}(t) &= (1 - |L_{\rm f}^{\rm CP}|^2)\cos\Delta m\,t + 2\Im L_{\rm f}^{\rm CP}\,\sin\Delta m\,t \end{aligned}$$

where the parameter, $L_{\rm f}^{\rm CP}$, is given by

$$L_{\rm f}^{\rm CP} = \frac{1}{\zeta}\frac{A_{\rm fCP}}{\overline{A}_{\rm fCP}}$$

and $A_{\mathrm{f^{CP}}}$ is the instantaneous decay amplitude for the B^0 or $\mathrm{B}^0_{\mathrm{s}} \to \mathrm{f}^{\mathrm{CP}}$ decays.

The decay rates $R_{\mathrm{f}}(t)$ and $\overline{R}_{\mathrm{f^{CP}}}(t)$ are for processes which are conjugate to each other and so are $\overline{R}_{\mathrm{f}}(t)$ and $R_{\mathrm{f^{CP}}}(t)$. If there exists any difference between $R_{\mathrm{f}}(t)$ and $\overline{R}_{\mathrm{f^{CP}}}(t)$ or $\overline{R}_{\mathrm{f}}(t)$ and $R_{\mathrm{f^{CP}}}(t)$, this is a clear sign of CP violation.

The final state f can be classified into the following four different cases:

I. Flavour specific final state

II. Flavour non-specific final state

II-a. CP eigenstate

II-b. mixed CP eigenstate

II-c. CP non-eigenstate.

4.1.4 CP Violation: Clean Case

The contributions to the B^0 decaying into $\mathrm{J}/\psi\,\mathrm{K_S}$ [2] are dominated by the tree diagram with $V^*_{\mathrm{cb}}V_{\mathrm{cs}}$. Although there exist some contribution from the $\mathrm{b} \to \mathrm{s} + \mathrm{c\overline{c}}$ penguin diagrams, the dominant penguin diagram contribution has the CKM phase $V^*_{\mathrm{tb}}V_{\mathrm{ts}}$ which is close to that of the tree diagram (Figure 11) [3]. Thus, we can safely assume that there is no CP violation in the decay amplitude and the ratio of the $\overline{\mathrm{B}}^0$ and B^0 decay amplitudes is given only by the CKM part. By noting that $CP(\mathrm{J}/\psi\,\mathrm{K_S}) = -1$ we obtain

$$\frac{A(\overline{\mathrm{B}}^0 \to \mathrm{J}/\psi\,\mathrm{K_S})}{A(\mathrm{B}^0 \to \mathrm{J}/\psi\,\mathrm{K_S})} = -\frac{(V^*_{\mathrm{cb}}V_{\mathrm{cs}}V^*_{\mathrm{us}}V_{\mathrm{ud}})^2}{|V^*_{\mathrm{cb}}V_{\mathrm{cs}}V^*_{\mathrm{us}}V_{\mathrm{ud}}|^2} \ .$$

Using the formulae developed in the previous section, the time dependent rates for the initial B^0 decaying into $\mathrm{J}/\psi\,\mathrm{K_S}$, $R_{\mathrm{J}/\psi\,\mathrm{K_S}}(t)$, and that for $\overline{\mathrm{B}}^0$ decaying into $\mathrm{J}/\psi\,\mathrm{K_S}$, $\overline{R}_{\mathrm{J}/\psi\,\mathrm{K_S}}(t)$ are given by

$$R_{\mathrm{J}/\psi\,\mathrm{K_S}}(t) \propto e^{-\bar{\Gamma}t}\left(1 + \Im\, L_{\mathrm{J}/\psi\,\mathrm{K_S}} \sin\Delta m\, t\right)$$
$$\overline{R}_{\mathrm{J}/\psi\,\mathrm{K_S}}(t) \propto e^{-\bar{\Gamma}t}\left(1 - \Im\, L_{\mathrm{J}/\psi\,\mathrm{K_S}} \sin\Delta m\, t\right)$$

which allow us to extract

$$\Im\, L_{\mathrm{J}/\psi\,\mathrm{K_S}} = \Im\left(\zeta \times \frac{A(\overline{\mathrm{B}}^0 \to \mathrm{J}/\psi\,\mathrm{K_S})}{A(\mathrm{B}^0 \to \mathrm{J}/\psi\,\mathrm{K_S})}\right) = -\Im\left[\frac{(V^*_{\mathrm{td}}V_{\mathrm{tb}}V^*_{\mathrm{cb}}V_{\mathrm{cs}}V^*_{\mathrm{us}}V_{\mathrm{ud}})^2}{|V^*_{\mathrm{td}}V_{\mathrm{tb}}V^*_{\mathrm{cb}}V_{\mathrm{cs}}V^*_{\mathrm{us}}V_{\mathrm{ud}}|^2}\right] \ .$$

[2] The same conclusion is valid to any CP eigenstates generated by the tree diagram $\mathrm{b} \to \mathrm{c} + \mathrm{W}^-$ with $\mathrm{W}^- \to \mathrm{s} + \overline{\mathrm{c}}$.

[3] This is no longer true between the $\mathrm{b} \to \mathrm{d} + \mathrm{c\overline{c}}$ penguin diagrams and the $\mathrm{b} \to \mathrm{c} + \mathrm{W}^-$ tree diagram with $\mathrm{W}^- \to \mathrm{d} + \overline{\mathrm{c}}$

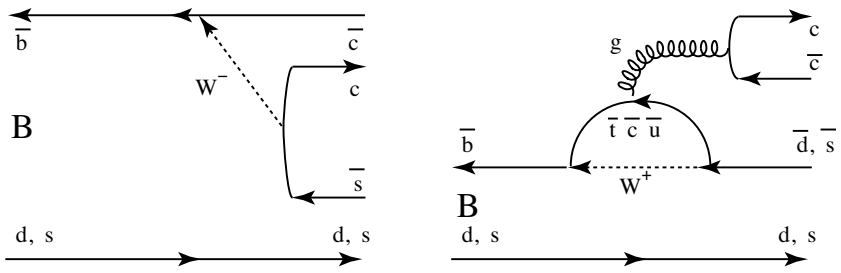

Figure 11: Tree and penguin diagrams contributing to the $\mathrm{B}^0 \to \mathrm{J}/\psi\,\mathrm{K_S}$ and $\mathrm{B}_\mathrm{s}^0 \to \mathrm{J}/\psi\,\phi$ decays.

With the Wolfenstein parameterization, it follows that

$$\Im\, L_{\mathrm{J}/\psi\,\mathrm{K_S}} = -\sin 2\beta \ .$$

The same argument holds for the $\mathrm{B_s} \to \mathrm{J}/\psi\,\phi$ decays and from the time dependent decay rates

$$R_{\mathrm{J}/\psi\,\phi}(t) \propto e^{-\bar{\Gamma}t}\left(\cosh\frac{\Delta\Gamma}{2}t + 2\Re\, L_{\mathrm{J}/\psi\,\phi}\sinh\frac{\Delta\Gamma}{2}t + \Im\, L_{\mathrm{J}/\psi\,\phi}\sin\Delta m\, t\right)$$
$$\overline{R}_{\mathrm{J}/\psi\,\phi}(t) \propto e^{-\bar{\Gamma}t}\left(\cosh\frac{\Delta\Gamma}{2}t + 2\Re\, L_{\mathrm{J}/\psi\,\phi}\sinh\frac{\Delta\Gamma}{2}t - \Im,\, L_{\mathrm{J}/\psi\,\phi}\sin\Delta m\, t\right)$$

one can extract

$$\Im\, L_{\mathrm{J}/\psi\,\phi} = \Im\left[\zeta \times \frac{A(\overline{\mathrm{B}}_\mathrm{s}^0 \to \mathrm{J}/\psi\,\phi)}{A(\mathrm{B}_\mathrm{s}^0 \to \mathrm{J}/\psi\,\phi)}\right] = -\sin 2\delta\gamma \ .$$

Note that we assumed in the calculation above that $CP(\mathrm{J}/\psi\,\phi) = +1$, i.e. the $\mathrm{J}/\psi\,\phi$ state is in the lowest orbital angular momentum state of $l = 0$. If there exists the $l = 1$ state with $CP(\mathrm{J}/\psi\,\phi) = -1$, the measured $\Im\, L_{\mathrm{J}/\psi\,\phi}$ will be diluted and the fraction of the $CP = -1$ state must be experimentally measured. If there is the same amount of $CP = +1$ state and $CP = -1$ state, $\Im\, L_{\mathrm{J}/\psi\,\phi}$ will vanish.

An even cleaner decay channel is $\mathrm{B}^0 \to \mathrm{D}^{*\mp}\pi^\pm$. There is only one tree diagram, $\overline{\mathrm{b}} \to \overline{\mathrm{c}} + \mathrm{W}^+$ followed by $\mathrm{W}^+ \to \mathrm{u} + \overline{\mathrm{d}}$, which contributes to the $\mathrm{B}^0 \to \mathrm{D}^{*-}\pi^+$ decays. The same final state can be produced from the $\overline{\mathrm{B}}^0$ decays with another tree diagram, $\mathrm{b} \to \mathrm{u} + \mathrm{W}^-$ followed by $\mathrm{W}^- \to \overline{\mathrm{c}} + \mathrm{d}$ (Figure 12). Therefore, the time dependent rate for the initial B^0 decaying into $\mathrm{D}^{*-}\pi^+$ is given by

$$R_{\mathrm{D}^{*-}}(t) \propto e^{-\bar{\Gamma}t}\left[1 + \frac{(1 - |L_{\mathrm{D}^{*-}\pi^+}|^2)}{(1 + |L_{\mathrm{D}^{*-}\pi^+}|^2)}\cos\Delta m\, t + \frac{2\Im L_{\mathrm{D}^{*-}\pi^+}}{(1 + |L_{\mathrm{D}^{*-}\pi^+}|^2)}\sin\Delta m\, t\right]$$

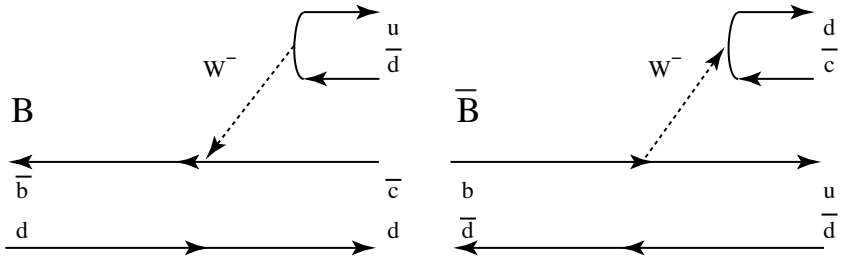

Figure 12: Tree diagrams contributing to the $B^0 \to D^{*-}\pi^+$ and $\overline{B}^0 \to D^{*-}\pi^+$ decays.

where

$$L_{D^{*-}\pi^+} = \zeta \times \frac{A(\overline{B}^0 \to D^{*-}\pi^+)}{A(B^0 \to D^{*-}\pi^+)} \ .$$

The weak phase of $A(\overline{B}^0 \to D^{*-}\pi^+)$ is given by $V_{ub}V_{cd}^*$ and that of $A(B^0 \to D^{*-}\pi^+)$ by $V_{cb}^*V_{ud}$. The phase of $L_{D^{*-}\pi^+}$ is then derived to be

$$\begin{aligned} \arg L_{D^{*-}\pi^+} &= \arg V_{ub} - \arg M_{12} + \varphi_S \\ &= -\gamma + 2\beta + \varphi_S \end{aligned}$$

where φ_S is a possible strong phase difference between the $b \to u + W^-$ and $\overline{b} \to \overline{c} + W^+$ tree diagrams.

CP-conjugated decay amplitudes of $A(\overline{B}^0 \to D^{*-}\pi^+)$ and $A(B^0 \to D^{*-}\pi^+)$, i.e. $A(B^0 \to D^{*+}\pi^-)$ and $A(\overline{B}^0 \to D^{*+}\pi^-)$ respectively, are obtained by taking the complex conjugate of the weak amplitudes while the strong phase remains unchanged. Thus for $D^{*+}\pi^-$ we obtain

$$R_{D^{*+}}(t) \propto e^{-\bar{\Gamma}t}\left[1 - \frac{(1-|L^{CP}_{D^{*-}\pi^+}|^2)}{(1+|L^{CP}_{D^{*-}\pi^+}|^2)}\cos\Delta m\, t - \frac{2\Im L^{CP}_{D^{*-}\pi^+}}{(1+|L^{CP}_{D^{*-}\pi^+}|^2)}\sin\Delta m\, t\right]$$

where

$$L^{CP}_{D^{*-}\pi^+} = \frac{1}{\zeta} \times \frac{A(B^0 \to D^{*+}\pi^-)}{A(\overline{B}^0 \to D^{*+}\pi^-)}$$

and the phase of $L^{CP}_{D^{*-}\pi^+}$ is given by

$$\begin{aligned} \arg L^{CP}_{D^{*-}\pi^+} &= -\arg V_{ub} + \arg M_{12} + \varphi_S \\ &= \gamma - 2\beta + \varphi_S \ . \end{aligned}$$

From the two time-dependent decay rates, we can extract $\gamma - 2\beta$ and φ_S.

Note that

$$|L_{\mathrm{D}^{*-}\pi^+}| = \left|L^{\mathrm{CP}}_{\mathrm{D}^{*-}\pi^+}\right| \approx \left|\frac{V_{\mathrm{ub}}V^*_{\mathrm{cd}}}{V^*_{\mathrm{cb}}V_{\mathrm{ud}}}\right| = \lambda^2\sqrt{\rho^2+\eta^2} \ll 1$$

i.e. the effect we have to measure is small.

The CP-conjugated time dependent decay rate distributions are given by

$$\overline{R}_{\mathrm{D}^{*+}}(t) \propto e^{-\bar{\Gamma}t}\left[1 + \frac{(1-|L^{\mathrm{CP}}_{\mathrm{D}^{*-}\pi^+}|^2)}{(1+|L^{\mathrm{CP}}_{\mathrm{D}^{*-}\pi^+}|^2)}\cos\Delta m\, t + \frac{2\Im L^{\mathrm{CP}}_{\mathrm{D}^{*-}\pi^+}}{(1+|L^{\mathrm{CP}}_{\mathrm{D}^{*-}\pi^+}|^2)}\sin\Delta m\, t\right]$$

and

$$\overline{R}_{\mathrm{D}^{*-}}(t) \propto e^{-\bar{\Gamma}t}\left[1 - \frac{(1-|L_{\mathrm{D}^{*-}\pi^+}|^2)}{(1+|L_{\mathrm{D}^{*-}\pi^+}|^2)}\cos\Delta m\, t - \frac{2\Im L_{\mathrm{D}^{*-}\pi^+}}{(1+|L_{\mathrm{D}^{*-}\pi^+}|^2)}\sin\Delta m\, t\right]$$

which can be used to obtain the same information.

A similar method can be used for the $\mathrm{B}^0_{\mathrm{s}} \to \mathrm{D}^{\mp}_{\mathrm{s}}\mathrm{K}^{\pm}$ decays to extract $\gamma - 2\delta\gamma$. The effect is larger since

$$|L_{\mathrm{D}^-_{\mathrm{s}}\mathrm{K}^+}| \approx \left|\frac{V_{\mathrm{ub}}V^*_{\mathrm{cs}}}{V^*_{\mathrm{cb}}V_{\mathrm{us}}}\right| = \sqrt{\rho^2+\eta^2} = O(1)\ .$$

4.1.5 CP Violation: Not So Clean Case

The penguin contribution to the $\mathrm{B_d} \to \pi^+\pi^-$ decay was originally thought to be small and the decay would be dominated by the $\mathrm{b} \to \mathrm{u} + \mathrm{W}$ tree diagram. However, the discovery of $B(\mathrm{B_d} \to \mathrm{K}^{\pm}\pi^{\mp}) > B(\mathrm{B_d} \to \pi^+\pi^-)$ indicates that the contribution of the penguin diagrams to the $\mathrm{B_d} \to \pi^+\pi^-$ amplitude should be $\sim 20\%$ or more.

Due to the penguin contribution, the phase of the $\mathrm{B}^0 \to \pi^+\pi^-$ decay amplitude deviates from that of V^*_{ub}. Furthermore, CP violation in the decay amplitude could be present. Evaluation of those effects involves calculating contributions from different diagrams accurately. Strong interactions may play an important role as well. Therefore, this decay mode may not be ideal to make precise determinations of ρ and η from CP violation.

4.2 Case with New Physics

Decay processes where only tree diagrams contribute should be unaffected by the presence of physics beyond the Standard Model. Therefore, $|V_{\mathrm{cb}}|$ and $|V_{\mathrm{ub}}|$ obtained from the semileptonic decays of B mesons would not be affected by the new physics and A and $\rho^2+\eta^2$ can be obtained even if physics beyond the Standard Model is present.

New physics could generate B^0-$\overline{B}^0$ and B_s^0-$\overline{B}_s^0$ oscillations by new particles generating new box diagrams. They could also generate a tree level flavour changing neutral current contributing to the oscillation. Since these contributions are through "virtual" states, they contribute to M_{12} with little effect on Γ_{12}, i.e.

$$M_{12} = M_{12}^{\rm SM} + M_{12}^{\rm NP},\ \Gamma_{12} = \Gamma_{12}^{\rm SM}$$

where $M_{12}^{\rm SM}$ and $\Gamma_{12}^{\rm SM}$ are due to the Standard Model and $M_{12}^{\rm NP}$ is the contribution from the new physics. The measured Δm is given by $2|M_{12}|$ and can no longer used to extract $|V_{\rm td}|^2$ due to $M_{12}^{\rm NP}$.

Since

$$\left|\frac{\Gamma_{12}}{M_{12}}\right| = \frac{2\left|\Gamma_{12}^{\rm SM}\right|}{\Delta m}$$

remains small, CP violation in the oscillation remains small as seen from Equation 57. Therefore,

$$\zeta = e^{-i\,\varphi_M}$$

is still valid. However, note that

$$\varphi_M \equiv \arg M_{12} \neq \arg M_{12}^{\rm SM}.$$

Decay amplitudes from the penguin diagrams can be affected by physics beyond the Standard Model since new particles can contribute virtually in the loop. Therefore, the modes such as B_d decaying into $\pi^+\pi^-$, $K^\pm\pi^\mp$ may have some contribution from the new physics.

Since the decays $B_d \to J/\psi\, K_S$ and $B_s \to J/\psi\,\phi$ are tree dominated, they are little affected by new physics. Therefore we have

$$\frac{A(\overline{B}^0 \to J/\psi\, K_S)}{A(B^0 \to J/\psi\, K_S)} = -\frac{A(\overline{B}_s^0 \to J/\psi\,\phi)}{A(B_s^0 \to J/\psi\,\phi)} = -1$$

with the phase convention due to the Wolfenstein parameterization and

$$L_{J/\psi\, K_S,\ J/\psi\,\phi} = \mp e^{-i\varphi_M}\ \ (- \text{ for } B_d \to J/\psi\, K_S \text{ and } + \text{ for } B_s \to J/\psi\,\phi)$$

and studies of the time dependent decay rates give $\arg M_{12}$.

The $B_d \to D^*\pi$ and $B_s \to D_sK$ decays are generated by only the tree diagrams and are not affected by new physics. Therefore we have

$$\arg L_{D^{*-}\pi^+} = -\gamma - \arg M_{12} + \varphi_S$$

and

$$\arg L_{D^{*+}\pi^-} = \gamma + \arg M_{12} + \varphi_S$$

and studies of the time dependent decay rates provide $\arg M_{12} + \gamma$. Similar studies can be made for $B_s \to D_s K$.

By combining the measurements of $B_d \to J/\psi\, K_S$ and $D^*\pi$ or $B_s \to J/\psi\, \phi$ and $D_s K$, the angle γ can be determined even in the presence of physics beyond the Standard Model. By comparing the result from B_d and that from B_s, consistency of the method can be tested. Since the phase of V_{ub} is given by γ and its modulus is measured from the semileptonic decay, ρ and η can be extracted. Once λ, A, ρ and η are known, M_{12}^{SM} can be calculated and from the measured Δm and $\arg M_{12}$, the new physics contribution M_{12}^{NP} is obtained. This can be used to identify the nature of the new physics contributing to the oscillation.

Whether new physics may contributes to the $b \to s + q\overline{q}$ penguin process can be examined by studying CP violation in B^0 and $\overline{B}^0$ decaying into ϕK_S where the decays are generated only by the penguin processes. In the Standard Model, the process is dominated by a loop with the virtual top quark, and the phase of the decay amplitude is given by V_{ts}: i.e. very small. Therefore, any large difference in the CP asymmetry from the $J/\psi\, K_S$ final state and that from the ϕK_S final state is a sign of new physics contributing to the penguin diagrams.

4.3 Experimental Status and Prospects

A possible experimental programme for the study of CP violation in the B meson system and search for physics beyond the Standard Model can be summarised in the following steps:

1. Determination of $|V_{cb}|$ and $|V_{ub}|$ from semileptonic (and some hadronic) decays,
2. Measurement of Δm for B_d and B_s,
3. Measurement of $\Im L_{J/\psi\, K_S}$,
4. Measurement of $L_{J/\psi\,\phi}$, $L_{D^{*\mp}\pi^{\pm}}$ and $L_{D_s^{\mp}K^{\pm}}$.

The first step has been made by ARGUS and CLEO at $\Upsilon(4S)$ machines and the four LEP experiments. BABAR and BELLE at the high luminosity asymmetric $\Upsilon(4S)$ machines are improving the precisions on those determinations. Future improvement of theory is also an important factor.

Half of the second step, $\Delta m(B_d)$ was done by ARGUS, CLEO, UA1, the four LEP experiments, SLD and CDF. For $\Delta m(B_s)$, we still have to wait for the results from CDF and D0. Already now four parameters of the CKM matrix are defined within the framework of the Standard Model, e.g. A, λ, ρ and η. Their accuracies will improve once Δm_s is measured.

Table 1: The current $\sin 2\beta$ measurements.

Experiments	$\sin 2\beta$	Reference
OPAL	$3.2^{+1.8}_{-2.0} \pm 0.5$	[29]
CDF	$0.79^{+0.41}_{-0.44}$	[30]
ALEPH	$0.84^{+0.82}_{-1.04} \pm 0.16$	[31]
BABAR	$0.741 \pm 0.067 \pm 0.033$	[32]
BELLE	$0.719 \pm 0.074 \pm 0.035$	[33]

The third step provides an additional information, $\beta = \tan^{-1} \eta/(1-\rho)$, within the framework of the Standard Model and consistency of the CKM picture can be tested. This step is now being made by BABAR, BELLE, and CDF and D0 will join the effort soon.

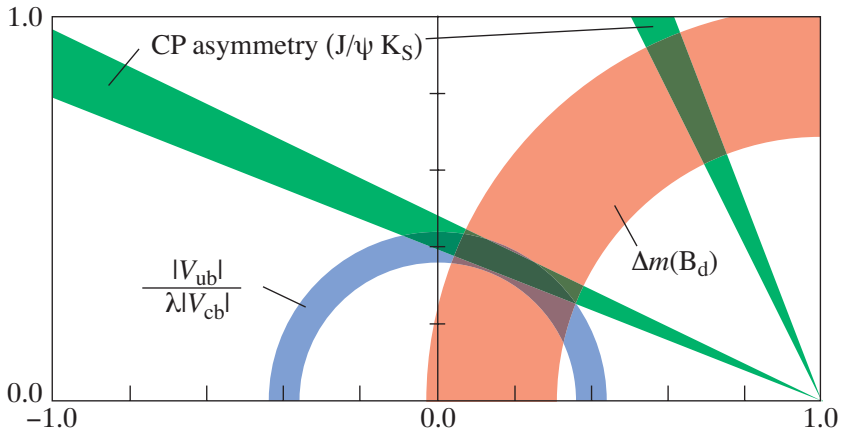

Figure 13: Regions in the $\tilde{\rho}$-$\tilde{\eta}$ plane allowed by the current measurements on $|V_{cb}|$, $|V_{ub}|$, Δm_d and $\sin 2\beta$.

Table 1 summarises the $\sin 2\beta$ measurements up to now. Both BABAR and BELLE experiments show that $\sin 2\beta$ is not equal to 0. By averaging the two measurements, where not only the $J/\psi\, K_S$ final state but also other CP eigenstates generated by the $b \to c + W^-$ process are used, we obtain

$$\sin 2\beta = 0.731 \pm 0.055 \ . \tag{61}$$

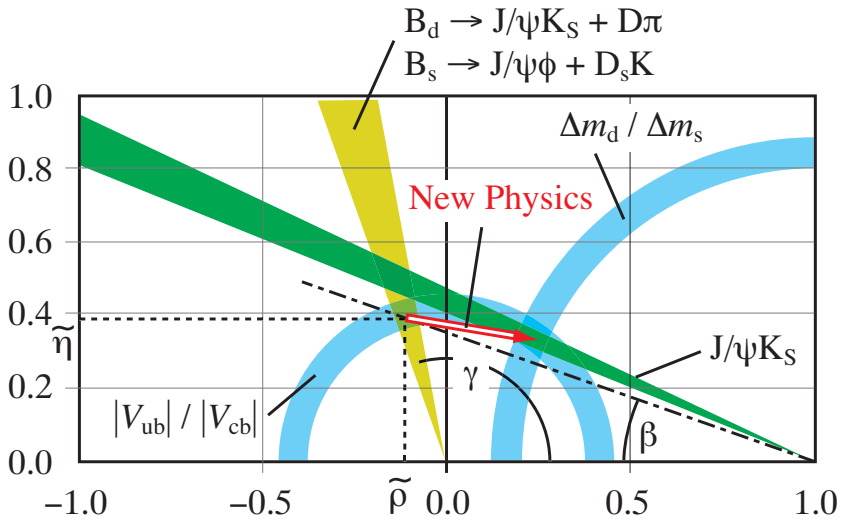

Figure 14: Possible situation of the allowed region in the $\tilde{\rho}$-$\tilde{\eta}$ plane after γ will be measured in $\sim$ 2007. It is also assumed that Δm_s will be measured by then. The contribution from new physics to the B^0-$\overline{B}^0$ oscillation is indicated.

The result clearly establishes CP violation in the B^0 and $\overline{B}^0$ decays.

Figure 13 shows a Standard Model analysis of $\tilde{\rho}$ and $\tilde{\eta}$ obtained from the B-meson system, i.e. $|V_{cb}|$, $|V_{ub}|$, Δm_d and $\sin 2\beta$ given by Equations 50, 59 and 61. Note that β from the $\sin 2\beta$ measurement has a twofold ambiguity.

It is remarkable that the regions given by the three equations overlap and a unique solution of $(\tilde{\rho},\ \tilde{\eta})$ can explain all the measurements. In conclusion, the current data can be consistently described by the Standard Model.

As demonstrated in the previous chapter, if physics beyond the Standard Model exists, the observed consistency with the Standard Model could be an accident where numerical cancellation is hiding new physics. The fourth step is needed to clearly examine the evidence of new physics and separate the effect due to the Standard Model and that from new physics if it exists. After the third step, only $\rho^2 + \eta^2$ will be known from $|V_{ub}|$ and the information on $\tan^{-1}\eta/(1-\rho)$ is spoiled by new physics. Only after the fourth step, ρ and η can be determined, together with isolating the new physics contribution.

For the last step, a new generation of experiments with statistics much higher than 10^{10} B mesons are needed. The B_s meson is an essential ingredient. After 2006, LHC will be the most powerful source of B mesons. Experiments must be equipped with a trigger efficient for hadronic decay modes to gain high statistics for

the necessary final states. Particle identification is also crucial in order to reduce background. LHCb is a detector at the LHC optimised for CP violation studies with B mesons. The two general purpose LHC detectors, ATLAS and CMS can contribute only to a limited aspect of the fourth step. BTeV at Tevatron could also make the last two steps. In this case, the theoretically clean determinations of γ outlined above will reveal new physics. After those studies, we may indeed find ourself in a situation shown in Figure 14 where γ is measured with an accuracy of $\pm 5^\circ$. It illustrates the case where the existence of new physics cannot be discovered from the CP asymmetry in the $J/\psi\, K_S$ final state alone.

Clearly CP violation is expected in many other decay channels. For many of them, there are some theoretical problems for making accurate predictions. However, they can be used to make a systematic study which will provide a global picture of whether CP violation can fit into the CKM picture. With all those experiments, we will continue to improve our understanding of CP violation and hope to discover physics beyond the Standard Model.

Acknowledgements

The author is very grateful to the organizers of this school for their extended hospitality and providing the stimulating atmosphere of the school.

References

[1] Wu, C.S. et al. (1957), *Phys. Rev.* **105**, 1413.

[2] Garwin, R.L et al. (1957), *Phys. Rev.* **105**, 1415,
Friedman, J.I. and Telegdi, V.L. (1957), *Phys. Rev.* **105**, 1681.

[3] Gell-Mann, M. and Feynmann, R.P. (1958), *Phys. Rev.* **109**, 193,
Sudarshan. E.C.G. and Marshak, R.E. (1958), *Phys. Rev.* **109**, 1860,
Sakurai, J. (1958), *Nuovo Cim.* **7**, 649.

[4] Christenson, J.H. et al. (1964), *Phys Rev. Lett.* **13**, 138.

[5] Aubert, B. et al. [(BABAR] (2001), *Phys. Rev. Lett.*, **87**, 091801.
Abe, K. et al. [BELLE] (2001), *Phys. Rev. Lett.*, **87**, 091802.

[6] Kobayashi, M. and Maskawa, K. (1972), *Prog. Theor. Phys.* **49**, 282.

[7] Cabibbo, N. (1963), *Phys. Rev. Lett.* **10**, 531,

[8] Sakharov, A.D. (1967), *JETP Lett.* **6**, 21.

[9] Kuzmin, V.A., Rubakov, V.A. and Shaposhnikov, M.E. (1985), *Phys. Lett.* **155B**, 36.

[10] Rummukainen, K. et al. (1998), *Nucl. Phys.* **B532**, 283.

[11] Shaposhnikov, M.E. (1986), *JETP Lett.* **44**, 364.

[12] For pioneering works see
Pais, A. and Treiman, S.B. (1975), *Phys. Rev.* **D12**, 2744,
Okun, L.B. et al (1975), *Lett. Nuovo Cimento* **13**, 218,
Bander, M. et al. (1979), *Phys. Rev. Lett.* **43**, 242,
Carter, A.B. and Sanda, A.I. (1981), *Phys. Rev.* **D23**, 1567,
Bigi, I.I. and Sanda, A.I. (1981), *Nucl. Phys.* **B193**, 85.

[13] More details can be found in
Nakada, T. (1991) *CP Violation in K- and B-Meson Decays*, PSI-PR-91-02.

[14] Weisskopf, V. and Wigner, E. (1930), *Z. fúr Physik* **63**, 54.

[15] Lüders, G. (1954), *Dan. Mat. Fys. Medd.* **28**, No5 ,
Pauli, W. (1995), *Niels Bohr and the development of physics*, ed. W. Pauli , pp. 30, New York, Pergamon Press,
Jost, R. (1975), *Helv. Phys. Acta* **30**, 409,
Lüder, G. (1957), *Annals of Physics* **2**, 1.

[16] K. Hagiwara et al. [Particle Data Group] (2002), *Phys. Rev.* **D66**, 010001

[17] Angelopoulos, A. et al. [CPLEAR] (1998), *Phys. Lett.* **B444**, 43.

[18] A. Alavi-Harati et al., (2002), *Phys. Rev. Lett.* **88**, 181601

[19] Apostolakis, A. et al. [CPLEAR] (1999), *Phys. Lett.* **B458**, 545.

[20] Ochs. W. (1991), MPI-Ph/Ph 91-35,

[21] Barr, G.D. et al. [NA31] (1993), *Phys. Lett.* **B317**, 233.

[22] Gibbons, L.K. et al. [E731] (1993), *Phys. Rev. Lett.* **70**, 1203.

[23] Alavi-Harati, A. et al. [KTeV] (2002), *Submitted for publication in Phys. Rev. D*, hep-ex/0208007

[24] Batley, J.R. et al. [NA48] (2002), *Accepted for publication in Phys. Lett. B*, CERN-EP/2002-061

[25] Wolfenstein, L. (1983), *Phys. Rev. Lett.* **51**, 1945.

[26] For details of the Standard Model description of the K and B system and further references, see the following articles:
Buras, A.J. (1998), *Weak Hamiltonian, CP violation and rare decays*, hep-ph/9806471,
Buras, A.J. (1999), *CP violation and rare decays of K and B mesons*, hep-ph/9905437.

[27] Buras, A. J., Parodi, F. and Stocchi, A. (2002), hep-ph/0207101.

[28] Alavi-Harati, A. et al. [The E799-II/KTeV] (2000), *Phys. Rev.* **D61**, 072006.

[29] Ackerstaff, K. et al. [OPAL] (1998), *Eur. Phys. J.* **C5**, 379.

[30] Affolder, T. et al. [CDF] (2000), *Phys. Rev.* **D61**, 072005.

[31] Barate, R. et al. [ALEPH] (2000), *Phys. Lett.* **B492**, 259.

[32] Aubert, B. et al. [BABAR] (2002), *Submitted for publication in Phys. Rev. Lett.*, hep-ex/0207042

[33] Abe, B. et al. [BELLE] (2002), *Submitted for publication in Phys. Rev. D*, hep-ex/0208025